Wang *et al. Energy Mater* 2024;4:400072
DOI: 10.20517/energymater.2024.39

Energy Materials

Review

Open Access

Check for updates

Covalent triazine frameworks (CTFs) drive innovative advances in rechargeable metal-ion batteries: a review

Zhuo Wang[1,2], Xiangyu Zou[1], Menglan Lv[1,*], Bin Zhang[1,*]

[1]Engineering Research Center for Energy Conversion and Storage Technology of Guizhou, School of Chemistry and Chemical Engineering, Guizhou University, Guiyang 550025, Guizhou, China.
[2]School of Chemical Engineering, Guizhou Institute of Technology, Guiyang 550003, Guizhou, China.

***Correspondence to:** Prof. Menglan Lv, Engineering Research Center for Energy Conversion and Storage Technology of Guizhou, School of Chemistry and Chemical Engineering, Guizhou University, No. 2708, South Section of Huaxi Avenue, Huaxi District, Guiyang 550025, Guizhou, China. E-mail: mllv@gzu.edu.cn; Prof. Bin Zhang, Engineering Research Center for Energy Conversion and Storage Technology of Guizhou, School of Chemistry and Chemical Engineering, Guizhou University, No. 2708, South Section of Huaxi Avenue, Huaxi District, Guiyang 550025, Guizhou, China. E-mail: zhangb@gzu.edu.cn

How to cite this article: Wang Z, Zou X, Lv M, Zhang B. Covalent triazine frameworks (CTFs) drive innovative advances in rechargeable metal-ion batteries: a review. *Energy Mater* 2024;4:400072. https://dx.doi.org/10.20517/energymater.2024.39

Received: 30 Apr 2024 **First Decision:** 31 May 2024 **Revised:** 21 Jun 2024 **Accepted:** 8 Jul 2024 **Published:** 30 Jul 2024

Academic Editor: Hao Liu **Copy Editor:** Fangling Lan **Production Editor:** Fangling Lan

Abstract

In the field of energy storage technology, the organic electrodes, separators, and electrolytes have unique advantages over inorganic materials, such as low cost, environmental friendliness, and a wide range of applications. Due to the advantages of organics such as light elements, abundant reserves, and recyclability, they have become favorable candidate materials for solving the energy storage problems caused by the fossil energy crisis. In recent years, as a high-performance branch of covalent organic frameworks, covalent triazine structures (CTFs) have attracted great interest due to their applications in electrochemical energy storage. CTFs have gradually become excellent organic materials for metal-ion batteries applications due to their large specific surface area, nitrogen richness, customizable structural features, and electron donor-acceptor/conductive parts. However, the relatively poor conductivity of the triazine ring in the main structure and the harsh polycondensation conditions limit its commercial application. To overcome these challenges, many effective strategies have emerged in terms of structural optimization, functional construction, and triazine-based composites. This review summarizes in detail the synthesis methods and applications of CTFs cathodes, electrolytes, and separators in the past decade. It is found that for CTFs, large-scale synthesis methods and performance regulation strategies have reached a bottleneck. It is hoped that the systematic summary of this review will provide strategic screening and prospects for the further expansion of CTFs research in next-generation batteries.

Keywords: Covalent triazine frameworks, organic cathode, electrolytes, separator, rechargeable metal-ion batteries

INTRODUCTION

Recently, the burgeoning energy crisis has caused the prices of crude oil and other commodities to rise continuously, in which the extent of its ecological damage and economic impact are worth pondering. As a result, the formidable challenge of energy scarcity has emerged as a pivotal concern for future scientific inquiry[1-4]. Currently, the most widely used pumped hydro energy storage method has the shortcomings due to its over-reliance on geographical location[5-7]. However, the energy storage batteries have become the best alternative due to their strong scalability, long lifetime, and high flexibility[8]. Within the realm of batteries, metal-ion batteries are distinguished by their substantial energy density and superior conversion efficacy, which exhibit strategic significance in mitigating the emissions of carbon dioxide (CO_2) and fortifying the foundations of energy security. In the 1970s, M.S. Whittingham harnessed titanium sulfide as the cathode and metallic lithium as the anode, thereby inventing the first lithium battery. Subsequently, in 1991, Sony commercialized the first lithium-ion batteries (LIBs) product[9-13]. With the continued strong demand in the new energy market and the release of production capacity in the industry, new batteries such as zinc ions[14], sodium ions[15], and lithium-sulfur[16] have appeared dramatically. During this period, scientific researchers conducted continuous research on the battery efficiency and found that it largely depended on the characteristics of the cathode materials[17].

At present, the cathode and anode materials of commercialized metal-ion batteries are mainly concentrated on inorganic materials. Among them, the cathode materials can be divided into hexagonal layered transition metal oxides ($LiTMO_2$, TM is one or more of Ni, Co, Mn), spinel compounds ($LiMn_2O_4$, $LiNi_{0.5}Mn_{1.5}O_4$, *etc.*), and polyanion compounds ($LiFePO_4$, $Li_3V_2(PO_4)_3$, $LiVPO_4F$, *etc.*) according to their crystal structure[18,19]. These inorganic materials have the dual characteristics of high electrochemical potential and low cost. However, they have a low theoretical capacity, high solubility, and are difficult to recycle. In particular, the sensitive electrolyte erodes the structure of inorganic cathode materials during battery operation, causing researchers to turn their attention to organic materials with stable structures[20-22]. In the 1960s, practical breakthroughs were made in the research on organic electrode materials (OEMs). Because the rechargeable LIBs based on carbon-based compounds were successfully constructed using three-carbon-based compounds as cathode materials, significant progress and confidence were brought to the field of OEMs[22,23]. Since 2008, organic electrodes have become a potential substitute for inorganic electrodes due to their structural tunability and low dielectric constant[24-28]. Among them, electrodes are designed and developed dramatically with porous covalent materials (PCM), such as covalent organic polymers (COPs) and frameworks (COFs). Their conjugated properties and porous structure promote the formation of highly exposed active sites in electrode materials, and effectively improve the energy storage capacity and cycle stability[29-31]. However, PCM electrodes are usually affected by stacked structure and easy degradation over time, which can readily lead to low conductivity and short cycling lifetime. Therefore, designing organic electrodes based on covalent triazine frameworks (CTFs) has become a highly feasible solution to solve the shortcomings of low conductivity and poor cycling stability in electrochemical energy storage[24,25,32,33].

Among the most of COFs, the CTFs are characterized by using aromatic rigid triazine (C_3N_3) as the building block to construct an organic framework by forming Schiff bases[34,35]. Through integrating heteroatoms such as oxygen, fluorine, sulfur, and carbon to forge bonds such as C-O, C-F, thiophene, and pyridine linkages, one can engender a plethora of functional groups, encompassing carboxyl (C=O), imine (C=N), and even azo (N=N) groups. Within a CTF possessing an array of these groups, the energy storage mechanism converts double bonds into single bonds through the incorporation of lithium ions (Li^+), triggering electron translocation within the molecular scaffold[36]. CTFs have no fragile linkages other than aromatic linkages, giving them excellent thermal and chemical stability. This inherent robustness enables

them to undergo one or more electron reductions throughout charge and discharge cycles, thereby endowing them with expansive realms of application and promising prospects[37]. However, traditional CTFs materials are generally prepared through methods such as ion heat or strong acid catalysis with harsh reaction conditions. So, most CTFs are produced in powder or film form[35], which limits production capacity and structural diversity design. Nevertheless, cathode materials predicated on CTFs are not without their deficiencies, such as the suboptimal exploitation of active sites and a diminished energy density, where these constraints impede the capacity of batteries to attain high-rate energy storage. To develop a universal CTFs synthesis method to provide a promising selection path for organic materials in metal-ion batteries[38], this review systematically summarizes the synthetic methods and cutting-edge applications of CTFs, to facilitate subsequent research on CTF-based cathode, electrolyte and separator materials.

SYNTHESIS METHODOLOGIES

In 2008, Kuhn and Thomas reported the first CTFs for the first time[39], where they used 1,4-dicyanobenzene (DCB) as the basic structural unit, and $ZnCl_2$ salt as the solvent and catalyst. This method requires a high-temperature process of more than 300 °C. After the emergence of this method, many strategies for synthesizing CTFs with various two- (2D) or three-dimensional (3D) structures were developed, such as super acid-catalyzed polymerization[40] and aromatic amide condensation[41]. Based upon the necessity of elevated thermal conditions, the synthesis methodologies can be broadly categorized into high- and low-temperature techniques: the ion thermal generation used by Kuhn *et al.* and the subsequent phosphorus pentoxide (P_2O_5)-involved methods are both high-temperature methods (> 300 °C)[39], while the condensation polymerization of aldehyde monomers and amidine monomers and the catalytic method under strong acid conditions are all carried out under low-temperature conditions (< 200 °C). This section will systematically discuss the preparation method of CTFs, including ionothermal trimerization at high temperature, P_2O_5 catalyzed at high temperature, polyphosphoric acid-catalyzed polymerization, super acid-catalyzed polymerization, amidine-based polycondensation and Friedel-Crafts reaction, as presented in Figure 1.

Ionothermal trimerization

Through the ionization heat synthesis route utilized in preparing CTFs, Kuhn *et al.* first synthesized CTF-1 through trimerization using DCB as the monomer and $ZnCl_2$ salt as the solvent[39]. At a high temperature of 400 °C, due to the Lewis acid-base interaction, the nitrile unit dissolves well in the molten ionic $ZnCl_2$ melt while gradually and spontaneously trimerizing through the intermolecular cyano groups. Under the catalysis of $ZnCl_2$ and high temperature, the reaction is fully reversible. Although high temperatures will cause certain decomposition of CTFs, they are still necessary. At temperatures below 400 °C, the aromatic compounds and heterocyclic nitrile monomers participating in the reaction are very stable. Only temperatures above 400 °C could promote their cracking and dehydrogenation to form condensation polymerization. CTF-1 is derived from readily available, cost-effective, and abundantly accessible aromatic nitriles, which possesses similar properties to molecular sieves (zeolites), COFs, and metal-organic frameworks (MOFs), namely high void content and high surface area (791 $m^2 g^{-1}$). Although the ionothermal synthesis method is easy to operate, it consumes high energy. To further optimize the synthesis strategy, Zhang *et al.* used the microwave method to enhance the generation of heat sources, which greatly reduced the time and energy consumption required for CTFs synthesis[42]. However, the reaction conditions were harsh, the operation was inconvenient, and the crystallinity of CTFs derivatives was poor. As a result, the subsequent application of this method has been limited.

Some harsh conditions, including elevated heating rates and temperatures, will inevitably cause carbonization of the product. Therefore, Lan *et al.* developed a low-temperature method by using a ternary

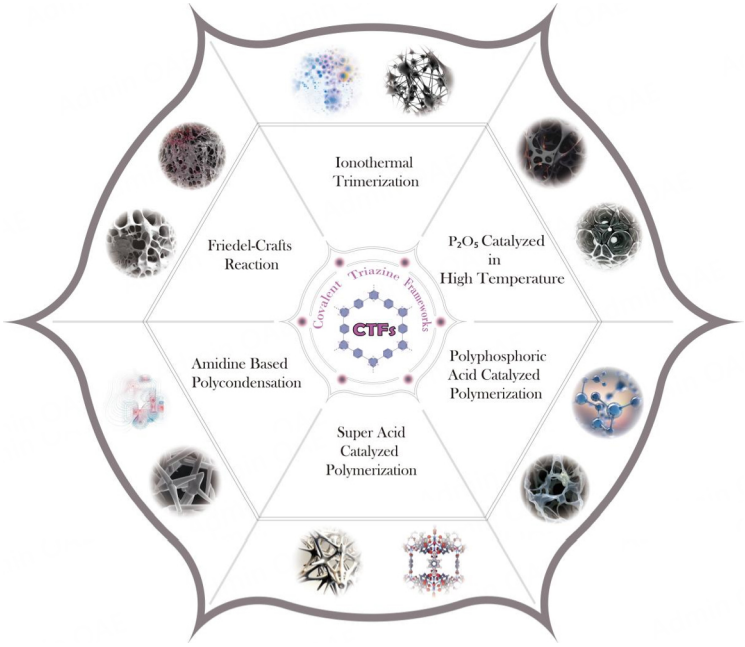

Figure 1. Summary of the synthesis methodologies of CTFs.

NaCl-KCl-$ZnCl_2$ mixture as a eutectic salt to prepare CTFs[43]. The melting point of the mixture hovers around 200 °C, significantly lower than the melting threshold of pure $ZnCl_2$ (318 °C). The low temperature overcomes the carbonation process associated with the final product, where the resulting material (CTF-ES200) exhibits superior photocatalytic efficacy relative to its counterpart CTF-1 by avoiding carbonization of the main polymer chain during the polycondensation process.

P_2O_5 catalyzed at high temperature

Even though the synthesis method using $ZnCl_2$ as a solvent is simple and feasible, the solvent itself is challenging to remove completely, and the presence of Zn ions may affect the further use of CTFs. Recently, Yu *et al.* proposed a method using P_2O_5 as a catalyst instead of $ZnCl_2$[41]. Meanwhile, aromatic amides such as benzamide were used to replace the precursors of nitrile benzene, and the triazine ring was prepared in two steps, as shown in Figure 2. Preliminarily, under the catalysis of P_2O_5, the aromatic amide group was converted into a nitrile group, and then a uniform triazine ring was formed through condensation. Surprisingly, the synthesis of the triazine derivative (*p*CTF-1) through this methodology yielded a heightened surface area (2,034 $m^2 g^{-1}$) and enhanced crystallinity. In addition, excess catalyst of P_2O_5 can be removed by simply mixing the product with water. This method makes it easier to remove the catalyst and is, therefore, more environmentally friendly than the classic $ZnCl_2$-based synthetic route. However, it still requires a higher temperature (> 400 °C), and the energy consumption is as high as ion thermal trimerization.

Polyphosphoric acid ($H_6P_4O_{13}$) catalyzed polymerization

In addition to the problem of high-temperature carbonization, both the traditional ionothermal and P_2O_5-catalyzed methods possess difficulties, such as low yield and poor crystallinity. To this end, Sun *et al.* creatively discovered that the catalytic employment of $H_6P_4O_{13}$ in the polymerization of CTFs presents a promising road[44]. The reaction mechanism included three steps: nucleophilic addition, cyclic addition, and acid separation. This method used aromatic nitriles as monomers to synthesize a series of high crystallinity CTFs at 300 °C. The microporous structure of these CTFs, with a high surface area from 794 to 1,335 $m^2 g^{-1}$,

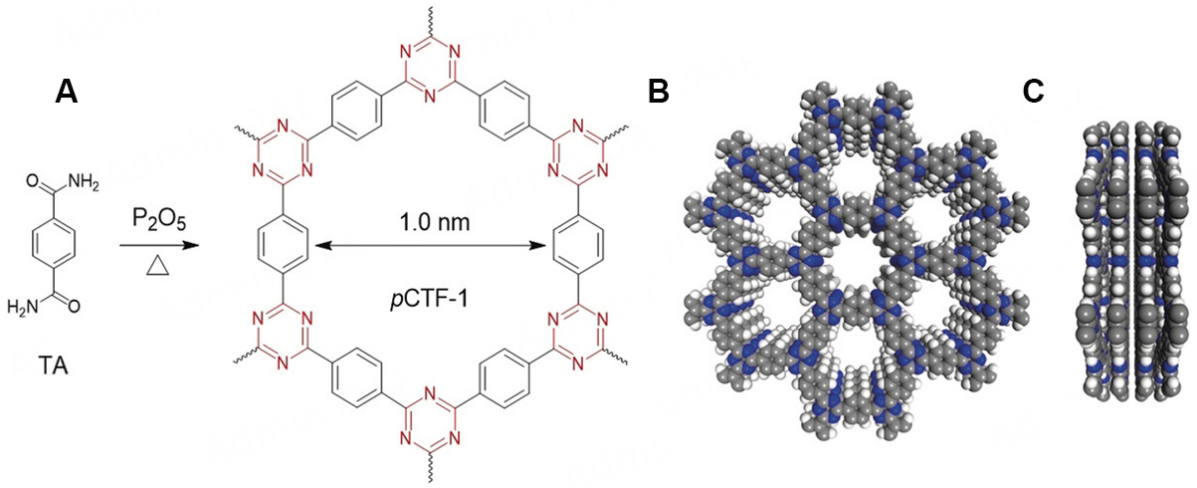

Figure 2. (A) Schematic diagram of the synthesis of pCTF-1. (B) Top view of the spatial structure of pCTF-1. (C) Side view of the spatial structure of pCTF-1. C: gray; N: blue; H: white[41]. Copyright 2018 John Wiley and Sons.

is much higher than most previously reported crystalline CTFs. Under the same conditions, only semi-crystalline or even amorphous CTFs can be obtained using H_3PO_4 and P_2O_5 as catalysts. This methodology exhibits a commendable level of operational simplicity, and $H_6P_4O_{13}$ is also cost-effective. However, this approach is scalable to the CTFs preparation on a kilogram scale, and the output is much higher than previously reported methods, providing the possibility for an industrial-scale application.

Super acid-catalyzed polymerization

It is well-known that the nitriles can be trimerized under the catalysis of strong Bronsted acids[40,45,46]. As early as 1966, Anderson *et al.* endeavored to employ chlorosulfonic acid as a catalyst for the trimerization of aromatic nitriles, aiming to synthesize *s*-triazine polymers[45]. In an effort to mitigate the carbonization attributed to the high-temperature synthesis, Ren *et al.* pioneered a technique operable at ambient temperature, utilizing a Bronsted acid to act as a catalyst[40]. This method utilized trifluoromethanesulfonic acid (TFMS) to trimerize aromatic nitrile monomers at room temperature into a series of CTFs (yield: 86%). The obtained product was no longer a black material (carbonized), but a free and amorphous light yellow fluorescent powder. However, the reaction time was long at room temperature, so they used the microwaves to heat the reaction vessel to 110 °C. Under microwave assistance, the reaction time was shortened from more than 4 h to less than 1 h, and the yield was significantly improved (yield: 96%). However, the crystallinity was still poor, and only some materials showed limited crystallinity. The surface area of these materials varied depending on the monomers (from 2 to 1,152 $m^2 g^{-1}$). This method successfully realizes the possibility of synthesizing CFT at low temperatures to avoid high energy consumption and carbonization. Subsequently, this approach has undergone refinement and optimization, leading to notable advancements, in which the synthetic strategies for non-carbonized CTFs have emerged for various applications, such as TFMS vapor-assisted[47,48] and interfacial polymerization methods[49-53]. In 2016, Huang *et al.* used a solid-phase mixture of nitrile monomer and closely packed SiO_2 nanoparticles to synthesize CTFs, by placing it in a sealed container and introducing TFMS vapor (100 °C) as catalysis [Figure 3][47]. Finally, after removing the silica template, the resulting polymer skeleton was solid and had no macropore collapse, resulting in a nanoporous polymer with a surface area of 90 $m^2 g^{-1}$. Compared with the traditional solvent method, the materials obtained by the steam-assisted method obtain an orderly connected hollow structure with the help of a tightly packed pore template and avoid carbonization at low temperatures. This proves that the TFMS vapor-assisted method can promote the formation of hollow nanostructures. Zhu *et al.* found that the

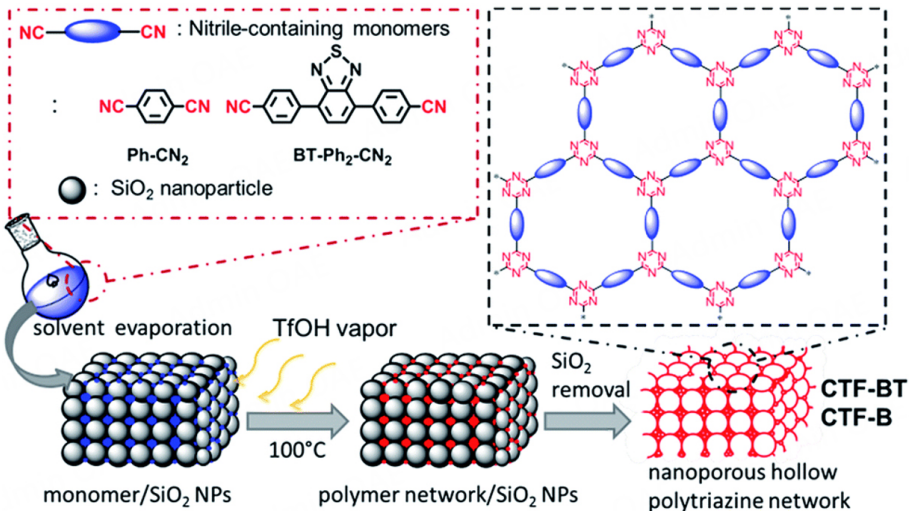

Figure 3. Schematic diagram of TFMS vapor-assisted synthesis of CTFs[47]. Copyright 2016 The Royal Society of Chemistry.

synthesized triazine materials can be easily prepared into films under low-temperature conditions[50]. After stirring the viscous solution of TFMS and 4,4'-biphenyl dicarbonitrile for 1.5 h, the mixed solution was then poured into a flat glass dish. By treating at 100 °C and washing away excess TFMS with an alkaline solution, a transparent and soft CTFs membrane (738 $m^2 g^{-1}$) can be easily obtained after drying. In this method, super acid as an essential component is still used to catalyze the occurrence of cross-polymerization. Although the above method avoids unnecessary decomposition and carbonization successfully, the reaction time is too long, leading to poor crystallinity. Liu *et al.* further improved the TFMS-based catalytic method to synthesize CTF-1 with high crystallinity successfully by introducing the interfacial polymerization method spontaneously[54].

It is noted that the super acid polymerization overcomes the disadvantages in high reaction temperature and long reaction time of the ionothermal synthesis method, which is beneficial to the synthetic operation. Moreover, to solve the problems of carbonization and decomposition of CTFs, low-temperature conditions are more conducive to directly obtaining film-typed materials. In addition, the safety hazards caused by the high toxicity of $ZnCl_2$ under high temperatures can also be eliminated. However, the catalyst used in this method is highly corrosive, and the large demand for solvents results in high costs. Therefore, it is still unclear whether this method can be transferred from laboratory milligram-scale synthesis to ton-scale production.

Amidine-based polycondensation

To further augment the synthesis scope whilst circumventing elevated thermal conditions or the employment of exceedingly strong acids, Wang *et al.* reported in 2017 a novel amidine-aldehyde polycondensation strategy to prepare various CTFs[55]. This methodology encompasses reversible Schiff base formation[56-59], Michael addition reaction[59-61], and irreversible processes of cyclization and dehydrogenation. Within the process of the Schiff base reaction, the aldehyde and amino groups undergo dehydration and condensation to forge an imine linkage. In the Michael addition reaction, the amino and the imine groups are deaminated and condensed to form a C=N double bond, and finally, a triazine unit is formed. This method uses dimethyl sulfoxide (DMSO) as the solvent, attributed to its weak oxidizing properties and high boiling point. In contrast, cesium carbonate (Cs_2CO_3) is used as the base due to its appropriate alkalinity. Ultimately, two kinds of monomers, including 1,4-benzene-dialdehye, 4,4′-biphenyl-

dialdehyde, tris(4-formylphenyl)-amine, and tris(4-formylbiphenyl)-amine, could react at 120 °C to get CTFs with bright colors, amorphous and layered structures, and high surface areas. Importantly, this method shows potential for scale-up synthesis since it only requires one-pot polymerization under mild conditions and does not involve strong acid or specialized equipment. Unfortunately, the crystallinity of the obtained material is still insufficient.

To solve the crystallinity problem of CTF, Liu *et al.* further developed a method to synthesize CTFs with higher crystallinity using an *in-situ* oxidation strategy in the following year[62]. In DMSO and alkaline solutions, alcohols can be slowly oxidized to aldehydes with air[63,64]. According to this strategy, the crystallinity of CTFs is greatly improved, allowing them to obtain higher thermal stability and layer structure. Meanwhile, the increase in crystallinity enables the materials to realize better charge transport capabilities and wider light absorption, which significantly improves the photocatalytic performance.

Friedel-crafts reaction

It is widely acknowledged that the classic Friedel-Crafts reaction has found extensive utility in the synthetic CTFs due to its low cost, mild conditions, effortless control, and reproducibility[65-68]. It involves cyanuric chloride and aromatic structural units as substrates, and under the action of catalysts such as anhydrous aluminum chloride and methanesulfonic acid (CH_3SO_3H), porous CTFs materials with favorable thermal and chemical stability can be realized[69-73].

One complex and deeply ingrained concept of the synthetic methods mentioned above is that the solvent is essential for the reaction, where the solvent promotes the interaction among the monomers involved in the reaction[74]. Therefore, mechanochemical method will be a time-saving, cost-effective and scalable alternative synthetic route[75,76]. In 2023, Krusenbaum *et al.* used mechanochemistry with the Friedel-Crafts alkylation method to eliminate the use of dangerous solutions and successfully synthesized triazine-based polymers with a specific surface area of more than 1,500 $m^2 g^{-1}$ in 1 min[77]. Significantly, the grinding of materials is critical to mechanochemical synthesis, which accelerates the direct progression of reactions. Moreover, the solvent-free allows the reaction to be freely observed, which provides a time-saving and scalable green solution for the synthesis of CTFs. However, the substitution of aromatic monomer sites in the Friedel-Crafts alkylation reaction is not the only selectivity, so the CTFs with the desired structure cannot be accurately constructed, and the structure obtained is often disordered.

In summary, the main methods for synthesizing CTFs can be roughly divided into high- and low-temperature methods. The high-temperature method has stringent requirements on equipment and cost, but it can produce CTFs with a clear structure and high specific surface area. The low-temperature method is more flexible and more scalable in industrial-level production, but due to the long reaction time at low temperatures and the dependence on solvents, the yield and crystallinity are always low. The specific method used for the synthesis of CTFs is mainly to be adjusted according to the physical and chemical properties such as the pore size, crystallinity, specific surface area, conductivity, *etc*. In addition, it is necessary to consider the basic properties of the monomers to avoid the loss of monomers during the reaction. Table 1 summarizes and compares the advantages and disadvantages of six common CTFs synthesis methods.

APPLICATION OF CTFS AS CATHODE MATERIALS

In contrast to traditional polymers, porous organic frameworks exhibit exceptional and distinct attributes. Owing to their robust networks, they enable the facile ingress of electrolyte ions. As an avant-garde class of porous polymers, CTFs are distinguished by their chemical stability, large specific surface area, and small

Table 1. Comparison of the advantages and disadvantages of CTFs synthesis methods

Synthesis methods	Advantages	Disadvantages
Ionothermal trimerization at high temperature	Economical catalysts, abundantly sourced, and excellent reactive properties	Partial carbonization of CTFs, generation of toxic gases, and residual Zn in the product
P_2O_5 catalyzed at high temperature	High specific surface area, high yield, and easier solvent removal	Partial carbonization of CTFs
$H_6P_4O_{13}$ catalyzed polymerization	Low cost, high crystallinity, and industrial production potential	High pollution and complex steps
Super acid-catalyzed polymerization	Mild conditions and short reaction time	Amorphous products, expensive equipment, low surface area and porosity
Amidine-based polycondensation	Mild conditions	Amorphous products
Friedel-Crafts reaction	Mild conditions, high specific surface area, and no hazardous solutions	Disordered structure and imprecise products

particle size. As a prospective material for cathode, CTFs proffer several advantages:

(1) The high conjugation of the polymer skeleton promotes electron transfer.

(2) The meticulously arranged nanopores afford a conducive environment for the efficient storage and controlled release of ions.

(3) The higher nitrogen content of the azine group provides a large amount of reaction sites.

The above advantages have led to many studies focusing on the application of composite materials in recent years. This section aims to encapsulate the substantial strides made in exploring the applications of CTFs cathodes across two key dimensions, corresponding to the energy storage materials of alkaline ion batteries, lithium-sulfur batteries (LSBs).

Alkaline-ion batteries

The alkaline-ion batteries with two active electrodes exhibit the disparate redox potentials to facilitate reversible redox reactions, and thereby accomplish charge and discharge cycles[78]. Throughout the discharge cycle, positive ions move from the anode to the cathode, a process that occurs simultaneously with the release of electrons. In contrast, during the charging phase, the directional flow of the reaction is reversed[79-81]. By selecting appropriate electrode materials and further optimizing their physical and chemical properties, the efficiency and cycling lifetime can be improved, thus promoting the further development of electrochemical energy storage technology[82,83]. The ion transport rate of the cathode material has also become one of the factors limiting the battery performance. Hence, the researchers are committed to developing efficient cathode materials with high ion transport rates and excellent electrochemical properties to improve the energy and power densities of batteries[84-88]. To understand the properties of metal-based batteries distinctly, the device performance is summarized in Table 2.

Lithium-ion batteries

Regarding the cathodes of LIBs, the commercialization of inorganic cathode materials (lithium manganate, lithium cobalt oxide ($LiCoO_2$), nickel-cobalt-manganese ternary composite, *etc.*) has been relatively mature. Both of high energy density and more than 30 years of market exploration have enabled it to dominate major markets such as electric vehicles and electronic equipment. However, current LIBs have almost reached the limit of energy density (based on volume and mass) of 750 Wh L^{-1}. Tesla's high-tension cylindrical 18,650 battery has reached about 600-650 Wh L^{-1} (20% reduction in the bag and prismatic battery

Table 2. Electrochemical performances of representative CTF-based metal-ion batteries

Main body	Types of batteries	Voltage range (V)	Current density (A g^{-1})	Cycles (retention rate)	Specific capacity (mA h g^{-1})	Ref.
Azo-CTF	LIBs	1.2-3.0	0.1	5,000 (89.1%)	205.6	[33]
CTF-P	LIBs	1.0-4.3	1.0	2,000 (78%)	78	[36]
CTF-P	LIBs	1.0-4.3	0.1	50 (79%)	135	[36]
CTF-P	LIBs	1.0-4.3	0.02		247	[36]
MPT-CTF@CNT	LIBs	1.5-4.2	0.4	60 (93%)	297	[38]
G-PPF-p-400-600	LIBs	1.5-4.5	5.0	5,100 (95%)	395	[91]
G-PPF-p-600	LIBs	1.5-4.5	0.4	400	255	[91]
G-PPF-p-600	LIBs	1.5-4.5	3.2	400	165	[91]
G-PPF-p-400	LIBs	1.5-4.5	0.4	400	155	[91]
G-PPF-p-400	LIBs	1.5-4.5	3.2	400	100	[91]
G-PPF-m-400	LIBs	1.5-4.5	0.4	400	125	[91]
G-PPF-p-400	LIBs	1.5-4.5	3.2	400	75	[91]
G-PPF-o-400	LIBs	1.5-4.5	0.4	400	55	[91]
G-PPF-p-400	LIBs	1.5-4.5	3.2	400	25	[91]
FCTF	LIBs	1.5-4.5	0.2	400 (88%)	106.3	[110]
FCTF	LIBs	1.5-4.5	0.1	200	125.6	[110]
BDMI-CTF	LIBs	1.5-4.5	1.0	2,000 (95%)	186.5	[114]
BDMI-CTF	LIBs	1.5-4.5	2		107.5	[114]
CTF-based-Mg	MIBs	0.8-2.4	5 C	3,000 (41.2%)	72	[122]
2D-NT-COF	AIBs	0.5-2.8	0.1	4,000 (97%)	132	[129]
TTPQ	ZIBs	0.1-1.4	0.3	250 (94%)	404	[133]
F-CQN-1-600	LIBs	1.5-4.5	2.0	2,000 (95.8%)	120	[183]
F-CQN-1-600	LIBs	1.5-4.5	5		105	[183]
F-CQN-1-600	LIBs	1.5-4.5	0.1		250	[183]
CTF-Az-400/600	LIBs	1.5-4.5	0.2	5,000 (95%)	118.5	[184]
CTF-800	LIBs	1.5-4.2	0.1	400 (88%)	116	[185]

configurations)[89]. The finite reserves of lithium confront boundless market demand, a challenge compounded by the scarcity of elemental resources such as cobalt and nickel. This dilemma is further exacerbated by the laborious and energy-intensive synthesis processes necessitated at elevated temperatures, alongside the environmental toxicity posed by alkali metals[90]. Hence, CTFs, as one of the extensively investigated organic porous materials, boast attributes of environmental friendliness, operational safety, and an absence of recycling dilemmas, offering a substitute for conventional cathode materials.

However, CTF-based cathode materials need to be developed in practical applications, such as low-rate performance, low energy density, and insufficient utilization of active sites. These issues limit the performance of LIBs, where the solutions need to be found to overcome these challenges. To this end, researchers have developed multiple strategies, including composite carbon-based materials, structure modification, and conductivity tuning. In 2014, Su *et al.* combined 2D graphene with CTFs for the first time and proposed a strategy to fix CTFs with customized pore structure through covalent bonding, achieving the optimal pore diameter (2.1 to 7.3 nm) and specific surface area (651 to 1,683 $m^2 g^{-1}$)[91]. The resulting 2D coupled graphene-porous polyaryltriazine-derived framework (G-PPF) successfully gave the outstanding cycling stability as a cathode for LIBs, exhibiting a rate performance of 395 mAh g^{-1} at 5 A g^{-1}. After over 5,000 cycles, it can still show an excellent rate performance of 135 mAh g^{-1} at a high current density (15 A g^{-1}). This phenomenon is mainly due to the strong coupling of CTFs to graphene, which effectively inhibits the dissolution of the cathode active material by the electrolyte. This strategy offers the excellent

prospects for using CTFs as nanohybrid electrodes in LIBs. The research on CTFs as cathode material for LIBs in the following three years seemed to have stalled. This may be mainly due to the low conductivity of CTFs with a clear triazine structure, resulting in unsatisfactory energy storage performance[92]. Although the microporous characteristics of CTFs increase the specific surface area, the monodisperse microporous structure of the original CTFs is not conducive to obtaining high-rate performance. Cheng pointed out that in the microstructure of the electrode material, macropores reduce the distance for ions to diffuse to the inner surface, mesopores reduce the resistance, micropores enhance the electric double-layer capacitance, and the porous structure increases the number of ion channels. Therefore, hierarchical porous materials (interconnected micropores, mesopores, and macropore structures) can significantly improve electrochemical performance compared to single-sized pore materials[93-96]. In 2018, Yuan *et al.* proposed an *in-situ* polymerization strategy for preparing CTF-1 on redox graphene (rGO) with different sizes and shapes, thereby realizing the nucleation site for regulating CTFs growth and inducing the formation of hierarchical micro-mesoporous structures[97]. The material obtained by polymerization at high temperatures (400 and 600 °C) for 20 h, labeled CTF-rGO-400-600, exhibits higher performance than mainstream inorganic cathode materials (e.g., $LiFePO_4$) at low current density (0.1 A g^{-1}) with a more competitive high reversible capacity of 235 mAh g^{-1}. After increasing the current density at 5 A g^{-1}, it can still show a stable capacity of 172 mAh g^{-1} after 2,500 cycles. Microscopic characterization proves that the 2D rGO has a good morphological combination with CTFs [Figure 4]. Through strong π-π intermolecular interactions and heat treatment-induced structural reorganization, the composite material has been successfully expanded from a single micropore to a multi-level hierarchical micro-mesoporous structure, reducing the micropore proportion while increasing the micropore proportion. A high surface area of 1,357.27 m^2 g^{-1} ensures the exposure of active sites and high ion accessibility. This strategy of constructing multi-level layered composite materials to obtain organic cathodes with high capacity and high rate in LIBs is a solution to break the research bottleneck for CTF-based cathode materials.

In the same year, Lei *et al.* used a mechanical exfoliation method to polish two high-temperature synthesized CTFs (CIN-1 and SNW-1) and carbon nanotubes (CNTs) under solvent-free conditions at room temperature[21]. These two exfoliated covalent organic CNT composites (E-CIN-1/CNT and E-SNW-1/CNT) finally obtained a graphite-like thin-layer 2D structure [Figure 5]. Interestingly, both covalent organic nanosheets (CONs) showed an initial decrease and then a rise in capacity during cycling tests. After a decrease in capacity during the first ten cycles, a significant capacity increase was observed for the E-CIN-1/CNT electrode, which finally remained stable within the 250th cycle, achieving a maximum reversible capacity of 1,005 mAh g^{-1}. Similarly, the capacity of E-SNW-1/CNT decreased in the first 50 cycles, and then increased slowly and ultimately settled at 920 mAh g^{-1}. Compared with the multi-layer stacked bulk structure, the exfoliated thin-layer CONs successfully shorten the diffusion path of ions/electrons due to the versatile surface exposure, where it is gradually activated to increase the active sites for Li^+ storage, forming better lithium diffusion kinetics[98-100].

To enhance the conductivity and overall efficacy of CTFs composites, carbonaceous materials such as CNTs and graphene are integrated into their matrix, which give the composite excellent electrical properties[97,101-103]. Mechanical exfoliation can cause changes in the stacking of 2D materials, thereby transforming bulk crystalline materials into single-layer 2D materials[24,104,105]. However, only one method cannot solve the problem of few active sites in CTF. Zhang *et al.* ever designed a multi-active CTF to improve anode performance in 2019[24]; however, the anode strategy was also difficult to implement in the cathode during synthesis. Until 2021, Zhao *et al.* obtained a CTFs (E-TP-COF) cathode material with C-O and C-N dual active centers by mechanically exfoliating polyimide and triazine-based few-layer COFs[106]. This method fully uses the insoluble characteristics of CTFs to avoid the dissolution threat caused by

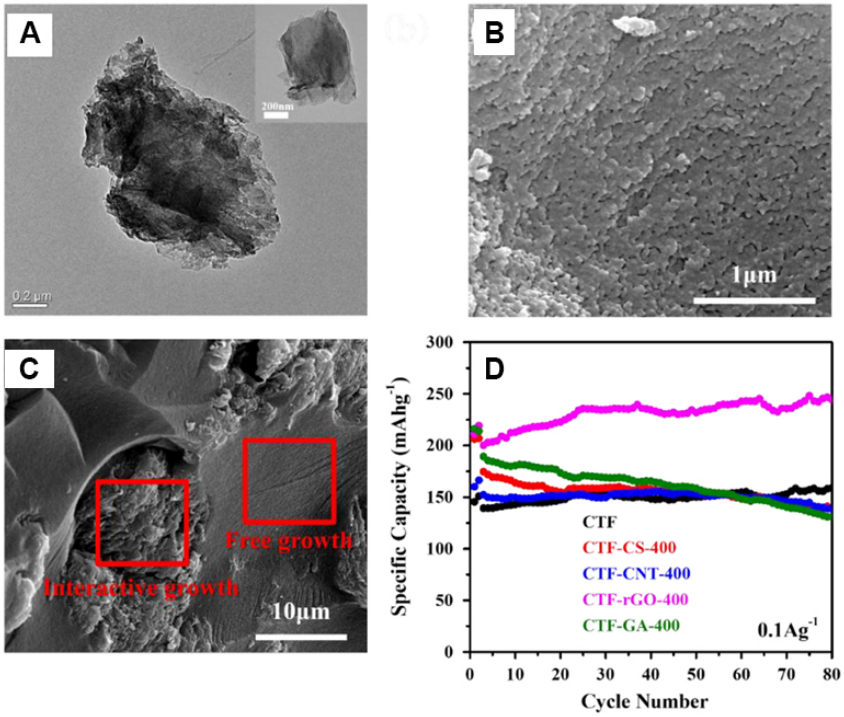

Figure 4. (A) TEM image of CTF-rGO composite cathode. (B) SEM image of CTF-rGO composite cathode. (C) SEM image of CTF-GA (Graphene aerogel) composite cathode. (D) Discharge capacity comparison at 0.1 A g^{-1} after 80 cycles[97]. Copyright 2018 Molecular Diversity Preservation International.

electrolytes, showing the excellent cycling stability. The dual active centers of C-N and C-O groups enable it to obtain a higher capacity than the pristine CTFs cathode with a single active center. To further verify the performance difference caused by structural changes, the exfoliated multi-layer nanosheet CTFs (E-TP-COF) and bulk CTFs (TP-COF) were tested under the same conditions. E-TP-COF showed a higher capacity of 110 mAh g^{-1} than 25 mAh g^{-1} of TP-COF, which means that the utilization of active sites during the stripping process is significantly enhanced.

Importantly, the molecular design is also the main starting point for changing the electrochemical properties of CTFs. The reactive functional groups, such as C=O, C=N, and N=N, could react reversibly with Li^+, triggering electron transfer through the reduction and transformation between double bonds and single bonds[107-109]. Wu *et al.* prepared an azo-linked CTF (Azo-CTF) by utilizing 4,4′,4″-(1,3,5-triazine-2,4,6-triyl) triphenylamine monomer (Tta) with undergoing an oxidative self-coupling reaction under the copper catalyst[33]. The Azo-CTF cathode used in LIBs presents a capacity retention rate of 89.1% after 5,000 cycles, and the capacity decay per cycle is only 0.00218%, showing ultra-long cycle life. When the current density is 0.1 A g^{-1}, it exhibits a reversible capacity of 205.6 mAh g^{-1}, and the capacity retention rate is as high as 84.4%. All of the six azo groups in Azo-CTF provide lithium insertion sites, and the strong adsorption of Li^+ by the nitrogen in the triazine ring, in which the azo-based functional groups are beneficial to the rapid diffusion of Li^+. Chen *et al.* used tetrafluoroterephthalonitrile ($C_8F_4N_2$) to fluorinate CTFs for improving their lithium storage performance[110]. When the resulting fluorinated CTF (FCTF) is used as a LIBs cathode, the FCTF simultaneously exhibits two redox reactions of n-type/p-type doping in stages, providing a maximum reversible capacity of 164.9 mAh g^{-1} (at 0.05 A g^{-1}). It can maintain 53% after 400 cycles at a current density of 200 mA g^{-1}, with a decay of 0.03% per cycle. Compared with nonfluorinated CTFs (135.1 mAh g^{-1} at 0.05 A g^{-1}), FCTF shows better electrochemical performance, proving that the

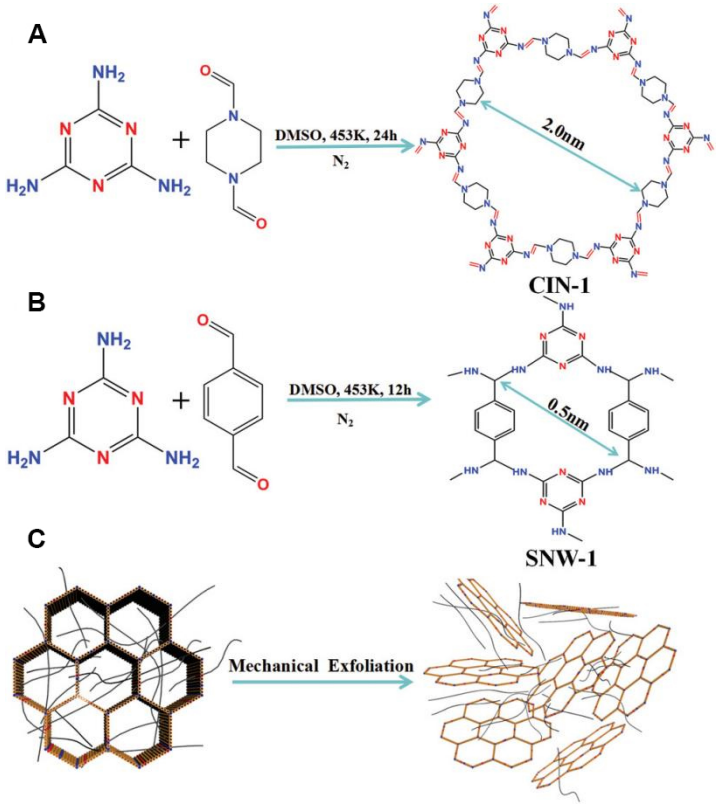

Figure 5. (A and B) Schematic diagram of the synthesis of CIN-1 and SNW-1. (C) Mechanical exfoliating process of CIN-1/CNT and SNW-1/CNT[21]. Copyright © 2019 John Wiley & Sons.

electron-withdrawing fluorine atoms can promote lithium storage. It is worth noting that the bipolar characteristics of the triazine ring allow the active sites of CTFs to be n- or p-doped during the charge and discharge process; however, the strong conjugation and tight layered structure of CTFs make the utilization rate extremely low. Affected by this, the ion transmission distance is longer, which is the main reason for unsatisfactory electrochemical performance[111-113]. Recently, Ren *et al.* took a new approach and selected monomers with different planarity, 7,7,8,8-tetracyanobenzoquinone dimethyl (TCNQ) and 1,3-bis(dicyanomethyl)indene (BDMI), to synthesize the modified CTFs (TCNQ-CTF and BDMI-CTF) with different spatial structure distortions through trimerization reaction [Figure 6][114]. As a cathode material for LIBs, it exhibits the highest initial capacity of 186.5 mAh g^{-1} at a low current density of 50 mA g^{-1}. In particular, it displays the extreme cycle stability at 1,000 mA g^{-1}, with a capacity retention rate of almost 100% after 2,000 cycles. Due to the more significant spatial distortion of the structure, the performance of BDMI-CTF is more robust than that of TCNQ-CTF. The proposal of this work provides a new method based on structural distortion for developing high-capacity and long-life OEMs.

Sodium-ion batteries

Due to the abundant reserves of sodium on earth and its similar chemical properties to lithium, sodium-ion batteries (SIBs) are considered as the mainstream product that is expected to replace LIBs in the next generation of batteries[115-117]. Because the atomic mass of sodium is higher than that of lithium, the energy density of SIBs is lower, implying that the weight and volume of SIBs are much larger than LIBs under the same energy density[118,119]. Till now, the CTFs are not widely used as cathode materials in SIBs, possibly resulting from low energy density of SIBs, but the characteristics of CTFs could stabilize the performance of

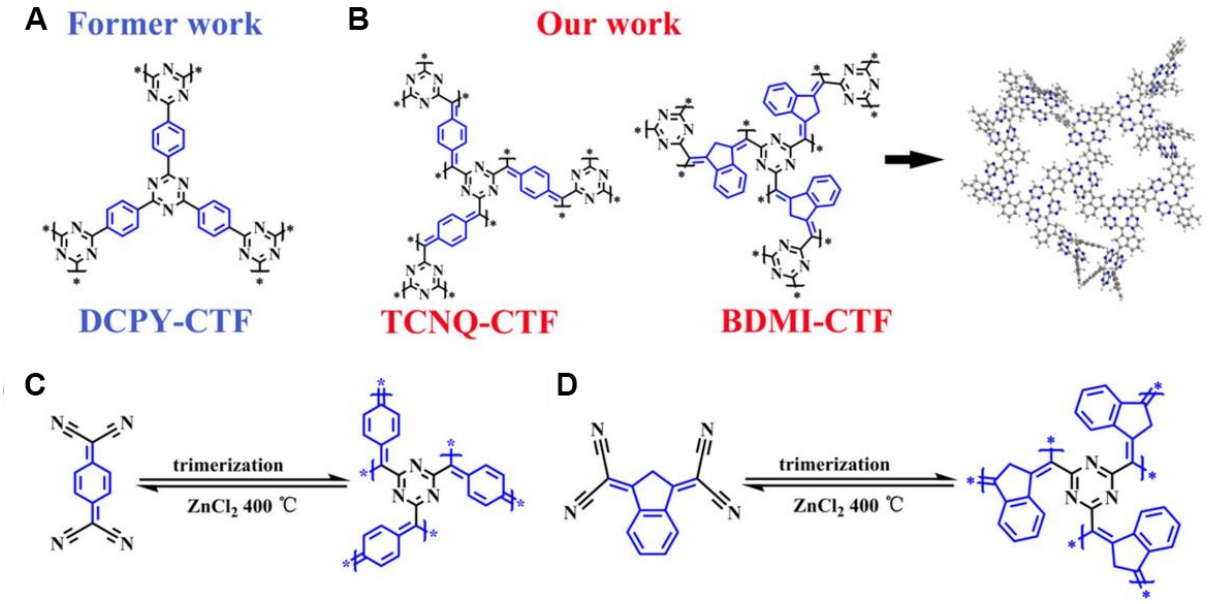

Figure 6. (A and B) Structural diagram of DCPY-CTF, TCNQ-CTF and BDMI-CTF. (C and D) Schematic diagram of the synthesis of TCNQ-CTF and BDMI-CTF[114]. Copyright 2024 Elsevier B.V.

SIBs potentially. In 2013, the application of CTFs in SIBs was first reported by Sakaushi by synthesizing a CTFs (BPOE) cathode composite material with a honeycomb skeleton using 2D aromatic and triazine rings[115]. The BPOE is a bipolar material that exhibits dual characteristics of n-type/p-type doping. At low current densities, a specific capacity of up to 200 mAh g^{-1} was demonstrated. Although the capacity is not high, the material is extremely stable. After 7,000 cycles at a high current density of 1.0 A g^{-1}, the capacity still retains 80% of the initial value. Li *et al.* used a simple polycondensation reaction to link 4,4′,4″-(1,3,5-triazine-2,4,6-triyl)trianiline (TAPT) with 1,4,5,8-naphthalenetracarboxylic dianhydride (NTCDA) and 1,2,4,5-benzenete-tracarboxylic anhydride (PMDA) to synthesize two different CTFs, respectively[120]. Moreover, it grew stably on CNTs to obtain TAPT-NTCDA@CNT and TAPT-PMDA@CNT. When used as a cathode material in SIBs, TAPT-NTCDA@CNT exhibits a specific capacity of 91.1 mAh g^{-1} (at 30 mA g^{-1}) and reasonable stability (capacity retention rate of 77% after 200 cycles). Recently, Shi *et al.* proposed a three-in-one (morphology control, molecular design, and post-synthetic vulcanization) strategy to synthesize a new 2D sulfide 2,4,6-Tris(4-aminophenyl)-1,3,5-triazine (S@TAPT-COFs/rGO) composite material, as shown in Figure 7[121]. Firstly, polyimide-based COF is stacked planarly through rGO to form 2D nanosheets; secondly, a triazine ring is introduced into the structure, replacing the amine as a monomer; finally, the obtained CTFs are sulfated using Lawesson's reagent to convert C=O into C=S, thereby enhancing the number of surface active sites. As a cathode material in SIBs, S@TAPT-COFs nanosheets demonstrated a specific capacity of 109.3 mAh g^{-1} at a current density of 0.1 A g^{-1} and still maintained 62.7% after 200 cycles at 2.0 A g^{-1}.

Other metal-ion batteries (Mg^{2+}, Al^{3+}, Zn^{+})

Recently, the magnesium, aluminum and zinc ions-based aqueous batteries have emerged as new metal-ion batteries. The anode of these metal-ion batteries is immutable, so the task of improving the performance of batteries falls on finding a suitable cathode urgently. The unique coordination mechanism of organic cathode materials can easily insert/deintercalate metal cations, but the problem of redox intermediate dissolution will cause rapid capacity decay. The polymeric rigid framework in CTFs is highly resistant to dissolution, and its structure and molecular design are more conducive to adjusting ion dynamics. Sun *et al.*

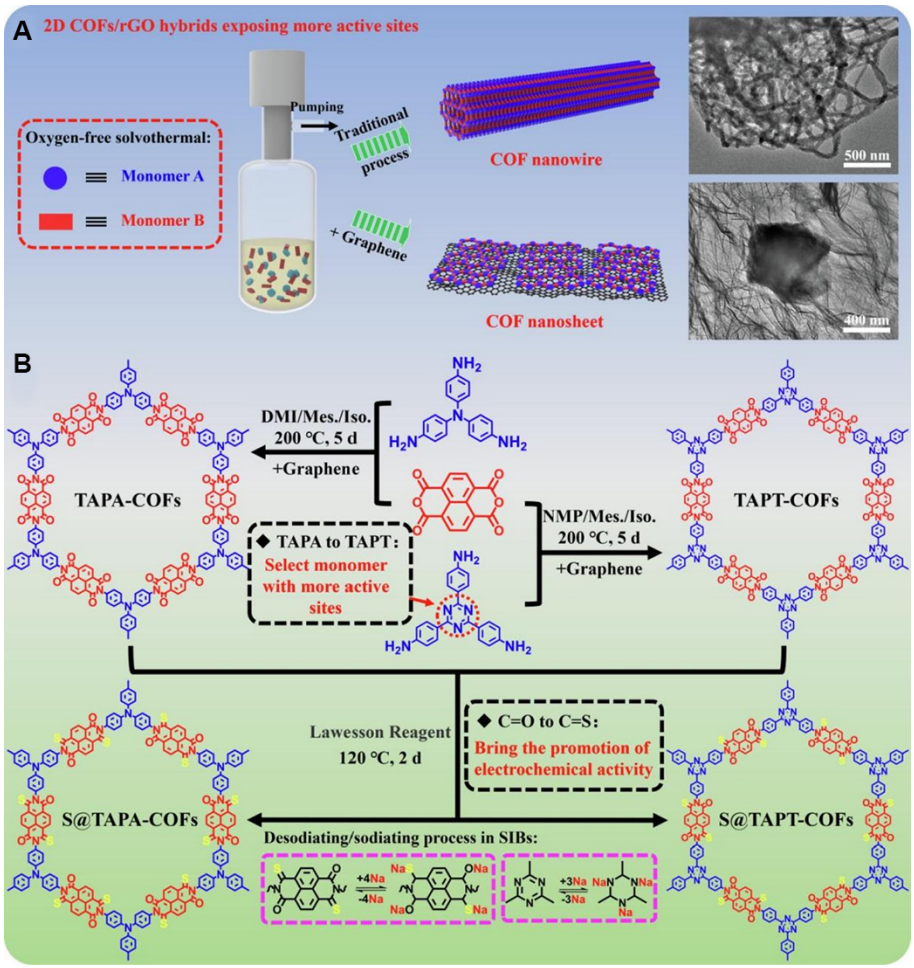

Figure 7. (A) Morphology control method of TAPA-COF. (B) Schematic diagram of the preparation, vulcanization and electrochemical mechanism of TAPA/TAPT-COF[121]. Copyright 2023 Elsevier B.V.

first attempted to use CTFs as a cathode material for magnesium-ion batteries (MIBs), where the resulting material was able to accommodate 9 Mg^{2+}[122]. They intended to use the highly ordered porous structure and large surface area of CTFs to increase the magnesium-ion diffusion rate and fully adapt to volume changes. The initial capacity of 102 mA h g^{-1} (at a current rate of 0.5 C) is not high, but its capacity only decays by 0.0196% after 3,000 cycles at a high rate of 5 C. This cycle stability is the best among reported organic MIBs[123,124], opening up the possibility for the application of porous polymers as high-performance OEMs in MIBs. Moreover, the aluminum metal batteries (AIBs) are considered as green and safe metal-ion batteries due to their non-flammable properties, high reserves, and nontoxic ionic liquids[125-127]. However, their low energy density and the complex dynamics of aluminum-based ions (Al^{3+}, $AlCl^{2+}$, $AlCl_2^+$, $AlCl_4^-$ and $Al_2Cl_7^-$) formed by the aluminum anode and electrode materials are the most difficult obstacles to their development[128]. Last year, Liu introduced the 4,4′,4″-(1,3,5-triazine-2,4,6-triyl)trianiline (TTTA) to the CTFs backbones to synthesize two kinds of 2D-COFs (2D-PT-COF and 2D-NT-COF) from pyromellitic dianhydride (PMDA) and 1,4,5,8-naphthalenetetracarboxylic dianhydride (NTCDA) successfully[129]. Among them, the 2D-NT-COF electrode achieved a maximum specific capacity of 132 mAh g^{-1}. This value is equivalent to the performance of CTFs in MIB cathodes, showing extremely high cycle stability. It can still maintain more than 97% of the initial capacity after 4,000 cycles, and the attenuation rate per cycle is only 0.0007%. Furthermore, the zinc metal is an abundant resource in the earth's crust with an abundance

reaching 79 ppm. Ranking fifth in global metal production, its market price is low. Notably, the zinc metal-based anode has good electrical conductivity and a theoretical capacity of 819 mAh g^{-1}, making it potentially applicable for commercialization. Attributing to the nontoxic, stable, low-cost, and high-capacity characteristics, zinc is believed to be one of the most ideal candidates for large-scale application in the next-generation secondary batteries. Moreover, the properties of zinc metal are highly compatible with neutral or near-neutral aqueous electrolyte systems, so aqueous zinc-ion batteries (AZIBs) have gradually received more and more attention[130-132]. It is widely known that the ionic conductivity of aqueous electrolyte is two orders of magnitude higher than that of organic electrolyte. However, the common inorganic cathode materials will cause volume expansion, structural damage, and other problems during operation, resulting in reduced capacity and stability of the battery system. In 2022, Wang *et al.* reported a new type of CTFs rich in quinone and pyrazine with the main skeleton comprising of quinoxalinophenazinedione and triazine, poly triazine-5,7,12,14-tetraaza-6,13-pentacenequinone (TTPQ)[133]. As a cathode material for AZIBs, it exhibits a high specific capacity of up to 404 mAh g^{-1} (at 0.3 A g^{-1}). After increasing the current density, it can still maintain 50% of the initial value (204 mAh g^{-1}). After 250 cycles, it can still maintain 94% of the charge and discharge capacity, with a single cycle attenuation of 0.024%. The TTPQ cathode exhibits a high specific capacity of 404 mAh g^{-1} at 0.3 A g^{-1} and maintains a specific capacity of 204 mAh g^{-1} at 5 A g^{-1} in AZIBs. The excellent rate performance is reflected in the capacity retention, which could remain approximately 82% of the initial capacity when the current density is gradually increased from 0.3 to 5 A g^{-1} and then back to 0.3 A g^{-1}.

In current commercial LIBs, the primary cathode materials employed are $LiCoO_2$, lithium manganese oxide ($LiMn_2O_4$), and lithium iron phosphate ($LiFePO_4$). The $LiCoO_2$, with a layered structure, serves as a cathode material and possesses a theoretical capacity of 274 mAh g^{-1}, displaying a practical highest capacity of up to 155 mAh g^{-1}. The $LiMn_2O_4$ features a spinel structure and offers a theoretical capacity of 148 mAh g^{-1}, with actual capacities ranging from 90 to 120 mAh g^{-1}. Meanwhile, $LiFePO_4$ has a theoretical capacity of 170 mAh g^{-1}, and its practical capacity can reach up to 145 mAh g^{-1} without the need for doping or modification[134]. In contemporary research, pure CTFs cathodes have achieved considerable practical capacities (refer to Table 2). Moreover, when combined with carbon-based materials such as graphene, the composite cathode materials exhibit higher capacities and more favorable operating voltages. Furthermore, regarding cyclic longevity, the materials such as G-PPF-p-400-600, F-CQN-1-600, CTF-P, and CTF-Az-400/600 demonstrate the capability to endure over 2,000 cycles while retaining more than 80% of their initial capacity.

Lithium-sulfur batteries

Because sulfur is a cheap and abundant non-metallic cathode active material, LSBs have garnered substantial attention and engendered widespread scholarly inquiry in recent years. LSBs generally consist of sulfur positive electrodes, lithium negative electrodes, electrolytes, and separators. During the discharge process, insoluble sulfur elements first combine with Li to form Li_2S_8 and then are further converted into soluble polysulfides (Li_xS) with different components. In this process, Li_xS shuttles the electrolyte, causing the battery volume to expand and subsequently pierce the membrane[135-139]. In addition, once Li_xS is produced by diffusion from the cathode, it is difficult to restore again in the form of lithium sulfide. So, the insoluble products often precipitate in the cathode and electrolyte, resulting in an irreversible reduction in battery cycle life[140,141]. To solve these problems, researchers have long been committed to developing technologies that can alleviate the shuttle effect in the past few years, including anode protection[142], separator strengthening[143], and electrolyte modification[144]. Compared with the traditional LIBs, sulfur has poor conductivity and requires carbon materials to improve its conductivity at the cathode. Therefore, another effective strategy is to sequester sulfur in carbon skeletons, especially porous carbon materials represented by mesoporous carbon[145], hollow carbon[146], and carbon nanospheres[147]. Owing to their

abundant pores, adjustable pore size, high specific surface area and designable functional groups, CTFs are also considered as an excellent host material for sulfur cathodes. They can anchor Li_xS in the middle by forming chemical solid bonds to prevent the shuttle effect. During the discharge process, it is combined with sulfur through covalent bonds, avoiding the dissolution and deposition of Li_xS. In addition, there are many optional monomers and strategies for constructing CTFs, which provides considerable flexibility for designing CTFs with different pore sizes and functional groups[148].

In 2014, Liao demonstrated the loading capacity of CTFs for sulfur cathodes for the first time[149]. They used a conventional ionothermal trimerization strategy to synthesize CTF-1 with a pore size of 1.23 nm from DCB under $ZnCl_2$ catalysis at 400 °C. After CTF-1 and sulfur were mixed at a mass ratio of 3:2, they were heated at a high temperature of 155 °C for 15 h through a melt diffusion strategy to obtain the composite material CTF-1/S@155 °C. At a rate of 0.1 C, a discharge capacity of 1,497 mA h g^{-1} was demonstrated in the first cycle. The capacity can remain at 762 mA h g^{-1} after 50 cycles (0.98% attenuation rate per cycle). To further compare and confirm the basal effect of CTF, they also prepared a simple mixture of CTF-1 and sulfur in the same ratio, CTF-1/S@RT. In contrast, CTF-1/S@RT exhibited poor initial capacity (1,015 mAh g^{-1}) and stability, with a discharge capacity as low as 480 mAh g^{-1} after only 20 cycles. The sufficient pore size of CTF-1 provides confinement space for sulfur, and the highly ordered 2D structure inhibits the dissolution of soluble Li_xS. However, the pore volume of CTF-1 is not large enough to complex large amounts of sulfur. The actual debt of sulfur is as low as 34 wt%, and cannot further limit the spread of Li_xS. In addition, CTF-1 itself does not have chemical adsorption of sulfur, and the improvement in electrochemical performance is mainly attributed to the spatial confinement effect. To surmount the challenge of limited sulfur loading capacity, Talapaneni developed an *in situ* vulcanization strategy of sulfur, using sulfur as a medium to condense DCB in elemental sulfur at a high temperature of 400 °C to form cyclic CTFs (S-CTF-1)[150]. When the elemental sulfur is dissolved at 160 °C, the material is subsequently heated to 400 °C, which triggers the ring-opening polymerization of sulfur into linear polysulfane. Fourier transform infrared spectroscopy (FT-IR) analysis found the stretching vibration peaks of C-S and S-S bonds, proving the formation of C-S bonds and the formation of polymerized sulfane within the framework of CTFs. Brunauer-Emmett-Teller (BET) analysis demonstrated that the original pores of S-CTF-1 were completely occupied by sulfur, showing that the material is non-porous and achieved a sulfur debt of 62 wt%. As an evaluation of sulfur cathode materials in LSBs, S-CTF-1 exhibits stable cycle performance. At a current density of 0.05 C, a discharge capacity of 482.2 mAh g^{-1} was obtained, maintaining 85.8% of the initial capacity after 300 cycles. Unlike physical bonds, the effect of strong sulfur bonds allows more sulfur to be stably and evenly distributed within the structure in the form of covalent attachment, thus effectively suppressing the shuttle effect. It is noted that the above strategies, whether through physical space constraints or C-S bond anchoring, still do not achieve high sulfur loading (both < 70 wt%)[151]. Moreover, the strategy developed by Talapaneni demonstrated the generation of ionic intermediates and free radicals from sulfur during high-temperature reactions. These intermediates can not only promote the formation of stable C-S bonds between the reaction intermediates and the aromatic monomers used to synthesize CTF, but also promote the trimerization of aryl cyanide to form CTF. Therefore, Je *et al.* followed this idea and envisioned via using the nucleophilic aromatic substitution reaction (S_NAr) between perfluoroaryl units and elemental sulfur to promote the increase of sulfur loading [Figure 8][152]. The fully conjugated polymer backbone (SF-CTF) was synthesized *in situ* through trimerization of perfluoroaryl cyanide and S_NAr reaction of sulfur. The remarkable effect is that this strategy has obtained a microporous framework with a sulfur content of up to 86 wt%, which means an effective increase in specific capacity (1,138.2 mAh g^{-1}, at 0.05 C). After 300 cycles, it can still maintain 81.6% of the initial value. Obviously, *in situ* sulfide is an effective strategy that can endow CTFs with higher chemical adsorption capacity of Li_xS. In 2019, Wang *et al.* followed the same strategy and selected the monomer 2,2′-[(perfluoro-1,4-phenylene) bis(methanyl-ylidene)] dimalononitrile (PPDN) to prepare fluorinated sulfur-rich multiple CTFs

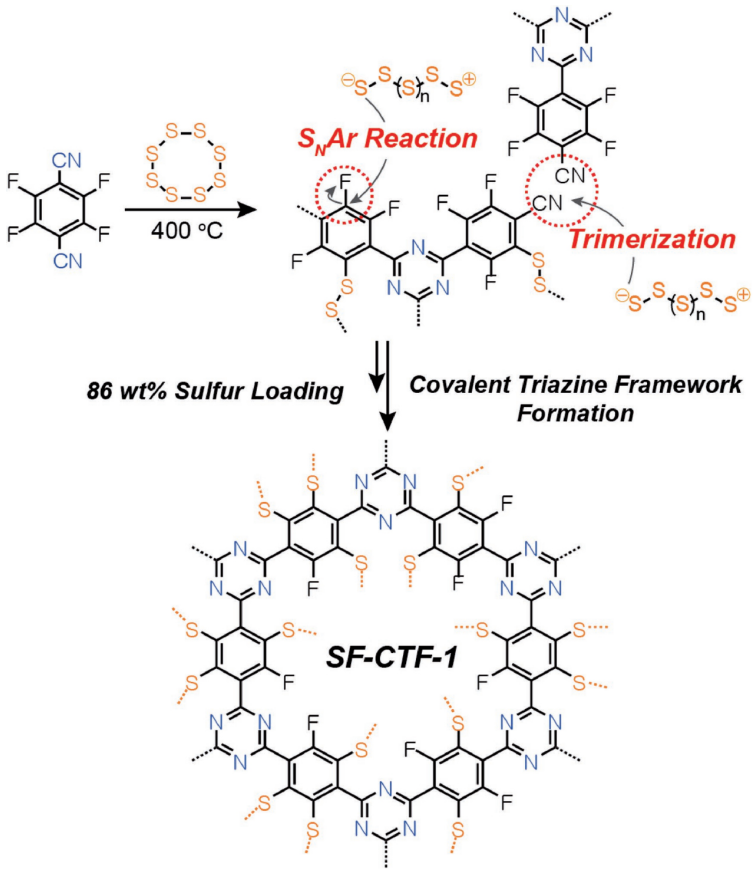

Figure 8. Schematic diagram of the synthesis of SF-CTF-1 and the S_NAr reaction process[152]. Copyright 2017 John Wiley & Sons.

(FMCTF-S), and obtained the similar results of performance[153]. This strategy further proves that *in situ* sulfide is a crucial and advantageous property for CTFs in LSBs, where the C-S covalent bonds and N-Li dipole-dipole interactions play an important role in the charge and discharge stability of sulfur cathode materials[154,155]. Taking advantage of the strong thiophilic property of allyl by introducing 5-(allyloxy) isophthalaldehyde and 4,4′,4″-(1,3,5-triazine-2,4,6-triyl) trianiline (TAPT) as comonomers, Li synthesized an allyl-rich CTFs (ART-COF)[156]. Although the sulfur loading (0.8 mg cm^{-2}) was not high, the ART-COF exhibited a highly stable lifetime and positive performance. The initial capacity could reach 1,270 mAh g^{-1}, where it can maintain 64% capacity after 500 cycles, and the Coulombic efficiency is close to 100%.

Even though the research progress has been made on how to increase the sulfur loading, there are few reports on the incorporation of heteroatoms into CTFs or the intentional functional design to improve the electrochemical performance of LSBs. Introducing functional groups with specific atom affinity into the structure of COFs is an effective method to weaken the shuttle effect caused by Li_xS, which could improve the performance of LSBs dramatically[157-160]. Inspired by this, Xiao *et al.* constructed a new boroxane-based structure that was both lithiophilic and sulfiphilic to stabilize the adsorption kinetics of Li_xS[161]. The boroxane unit can capture Li_xS through sulfophilic interactions, while the triazine ring can chemically absorb Li^+ through a large number of nitrogen atoms provided by C=N bonds. However, forming two reversible covalent bonds simultaneously was difficult due to mutual interference, and constructing bifunctional CTFs from a single monomer presents a challenge. Xiao *et al.* synthesized a CTFs derivative (TB-COF) containing triazine and boroxine units by using 4-cyanophenylboronic acid for self-

condensation[161]. After 800 cycles, the TB-COF/S electrode exhibited a reversible capacity of 663 mAh g^{-1} at a charge-discharge rate of 1 C, and the average capacity decay rate per cycle was only 0.023%. With a similar idea, Liang *et al.* prepared a CTF (COF-Tr-BA) with a pore diameter of 2.61 nm and a specific surface area of 650 m^2 g^{-1} by introducing the boronic acid group (4-ethynylphenyl) into the COF-Tr through the Diels-Alder cycloaddition reaction [Figure 9][162,163]. The interaction between the N atoms of the quinoline and triazine moieties on the main chain alleviates the dissolution of Li_xS and reduces the shuttle effect. The first discharge capacity is as high as 1,349 mAh g^{-1}, and the discharge capacity can still be maintained at 46% after 200 cycles. Zhang *et al.* also used a heteroatom doping strategy to construct a CTF containing N and O structural units (NO-CTF)[164]. The NO-CTF material exhibits a large surface area and pore volume, enabling the loading of a high sulfur content (4.8 mg cm^{-2}). Additionally, it provides expedited pathways for both electron and Li^+ transport, thereby enhancing the rate capability of the system, as evidenced by a capacity of 678 mAh g^{-1} at a rate of 2 C. Moreover, the uniform distribution of *N* and *O* heteroatoms in NO-CTF facilitates a strong interaction with lithium Li_xS, thereby accelerating their conversion and improving cycling stability and capacity, respectively.

The integration of conductive materials, including CNTs, graphene, and conductive polymers, into CTF-based electrode structures, represents a promising avenue for enhancing electron conductivity and optimizing electrochemical performance. The introduction of these conductive additives facilitates efficient electron transport and promotes the utilization of active sulfur species during the charge-discharge processes. Moreover, the utilization of metal-modified CTFs and carbon composite architectures has emerged as a compelling solution for mitigating the notorious "shuttle effect" phenomenon, referring to the undesirable migration of Li_xS intermediates in LSBs. This innovative approach exhibits pronounced potential in suppressing Li_xS dissolution, inhibiting shuttle processes, and consequently, improving the cycling stability, coulombic efficiency, and overall energy storage performance of LSBs systems. Gomes and Bhattacharyya used molecular engineering to synthesize new CTFs composite nanosheets (CNT-CON) by functionalizing multi-walled CNT with triazine and crystallizing COF[165]. Benefiting from the synergistic effect of CNT and CON trapping mechanisms, non-polar sulfur is confined by CNTs. In contrast, polar Li_xS is trapped by the 'chemical traps' in the CON framework. The cycle performance of CNT-CON/S is much better than that of sulfur-containing bare COF/S and sulfur-loaded bare CNT/S, achieving a first discharge capacity of up to 1,353 mAh g^{-1}. In 2020, Guan *et al.* grew *N* and *O* atom-rich diazinone-based CTFs *in situ* onto rGO through sulfur-mediated cyclization of dinitrile monomers, forming a ternary composite electrode (S/P-CTF@rGO)[103]. Owing to the nanopore structure, polar groups in nazinone and triazine, and conductive rGO, the specific capacity of the S/P-CTFs@rGO cathode can initially reach 1,130 mAh g^{-1}, where it can remain at 920 mAh g^{-1} (81.4%) after 500 cycles. Compared with the S/P-CTFs cathode without rGO, the S/P-CTFs@rGO cathode can provide higher capacity at high current rates. This impressive initial specific capacity of 1,130 mAh g^{-1} indicates that the efficient charge transfer and substantial utilization of active sulfur species are carried out sufficiently. Furthermore, even at a current rate of 0.5 C, the S/P-CTFs@rGO cathode consistently maintains a specific capacity of 1,130 mAh g^{-1}. After 500 cycles, it exhibits considerable capacity retention, with a specific capacity of 920 mAh g^{-1} (81.4%). Comparatively, the S/P-CTFs@rGO cathode outperforms the S/P-CTFs without rGO, particularly in terms of providing higher capacity under a high current rate. These findings underscore the superiority of the S/P-CTFs@rGO cathode in achieving enhanced capacity and stability, making it a candidate for high-rate applications in advanced energy storage systems. In addition to carbon-based materials, conductive polymers are another suitable additive to improve the conductivity of CTFs[166,167]. Kim *et al.* synthesized a CTF with ultra-high sulfur loading (83 wt%) from charged polypyrrole (cPpy) in the presence of elemental sulfur (cPpy-S-CTF) [Figure 10][16]. The introduction of cPpy enables cPpy-S-CTF to obtain high-affinity anchoring sites for Li_xS, good conductivity and promoted 3D nanochannels. Table 3 summarizes the reported performance on CTFs for LSBs in the past decade.

Table 3. Summary of the electrochemical performance of representative CTF-based LSBs

Main body	Sulfur loading (wt%)	Voltage range (V)	Current density (C)	Cycles (retention rate)	Specific capacity (mA h g^{-1})	Ref.
cPpy-S-CTF	83	1.8-2.8	0.05	500 (86.8%)	1,203.4	[16]
S/P-CTF@rGO	70%	1.7-2.8	0.5	500 (81.4%)	1,130	[103]
CTF-1/S@155 °C	34	1.1-3.0	0.1	50 (64%)	1,197	[149]
S-CTF-1	62	1.7-2.7	1	300 (85.8%)	562	[150]
SF-CTF	86	1.8-2.7	0.05	300 (81.6%)	1,138.2	[152]
FMCTF-S	77	1.6-3.0	1	400 (62.6%)	681	[153]
ART-COF/S	62	1.8-2.7	0.2	100 (96%)	1,270	[156]
ART-COF/S	62	1.8-2.7	1	500 (82%)	993	[156]
TB-COF	40	1.5-3.0	0.1	150 (71%)	1,044	[161]
COF-Tr-BA@S	40	1.7-2.8	0.5	200 (46%)	1,349	[162]
NO-CTF-1/S	71	1.5-3.0	0.5	300 (92%)	1,250	[164]
CNT-CON/S	78	1.0-3.0	0.5	50 (75%)	1,353	[165]
GPF-S-3	63	1.7-2.8	2	120 (66%)	1,461	[186]
FCTF-S	53%	1.7-2.8	0.1	150 (73.7%)	1,130	[187]
CTF-Celgard	60	1.7-2.8	1	800 (58.4%)	1,672	[180]
S/FCTF-400	62	1.7-2.8	0.5	200 (66.7%)	741	[188]
FLC	2.2 mg cm^{-2}	1.8-3.0	1	1,000 (63%)	792	[189]
OLC	2.2 mg cm^{-2}	1.8-3.0	1	1,000 (44%)	723	[189]
S@CTF-Mono	22	1.2-3.0	0.1	200 (41%)	2,582	[190]
S@CTF-Bi	26	1.2-3.0	0.1	200 (34%)	1,053	[190]
S-NC	1.8 mg cm^{-2}	1.7-2.8	1	80 (99.12%)	931.8	[191]
S@EB-COF-PS	71.70%	1.6-3.0	4	300 (41%)	1,136	[192]
S@CTF/TNS	76	1.5-2.8	1	1,000 (86%)	748	[193]
COF-SQ-Ph-S	80	1.7-2.8	0.5	150 (46%)	1,331	[194]
S@CTFO	67	1.7-2.8	1	300 (65%)	791	[195]
Co-CMP	16	1.7-2.8	0.5	1,000 (55%)	1,404	[196]
POP@F/S	71.5	1.8-2.7	0.5	500 (90.5%)	956.6	[197]
STP	5 mg cm^{-2}	1.6-2.8	0.5	150 (79%)	588	[198]
CoS_2-HUT-8/S	61	1.6-2.8	1	500 (77%)	757	[199]
CMP-M		1.7-2.8	0.5	1,000 (55%)	916	[200]
S@THZ-DMTD	82	1.6-2.8	1	200 (77.8%)	1,149	[201]
i-SCTF	60.53%	1.5-3.0	0.1	1,000 (89%)	1,146	[202]

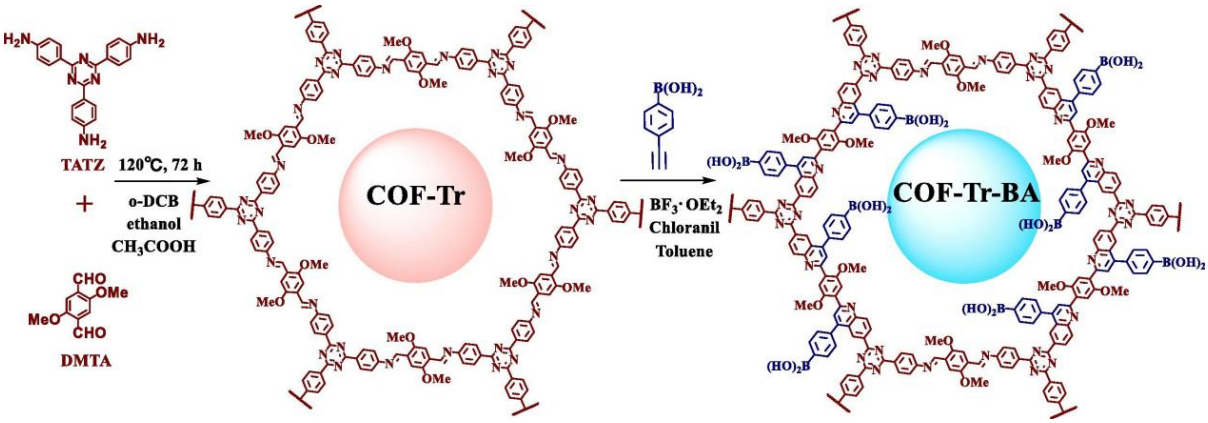

Figure 9. Schematic diagram of the synthetic route of COF-Tr-BA[162]. Copyright 2023 Elsevier B.V.

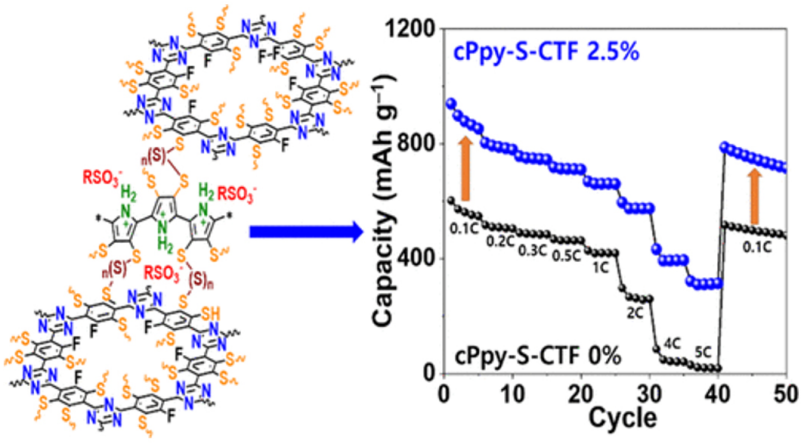

Figure 10. The structure, mechanism of action and electrochemical performance of cPpy-S-CTF[16]. Copyright 2020 American Chemical Society.

Performance improvement strategies

Based on the above research results, the performance enhancement strategies for CTFs in cathode materials focus on the following aspects:

(1) Composite with carbon-based materials: The nitrogen-rich properties of CTFs provide considerable chemical properties, but their inherent 2D structure, structural overlap and low conductivity limit the performance improvement. To solve the problem of low conductivity, an efficient way is to composite with carbon-based materials, such as graphene, rGO, CNTs and other materials. This allows the one-dimensional microporous structure to develop into a multi-level hierarchical micro-mesoporous structure, reducing the micropore ratio while increasing the micropore ratio. Moreover, the micropores enhance the double-layer capacitance, and the porous structure increases the number of ion channels. However, adding conductive carbon materials to CTFs composites will reduce the total energy density of the original CTFs.

(2) Structure functionalization: The redox reaction of metal-ion batteries during the charge and discharge process is the process of reversible cation/proton insertion and extraction of positive and negative electrodes and electron migration in the external circuit. CTFs have abundant redox active sites that can interact with metal cations and generate capacity through cation/proton insertion mechanisms during the redox reaction. The introduction of active functional groups into CTFs is an effective strategy to regulate ion transport efficiency, and improve ion conductivity and cation transfer number. So far, there are two main methods to introduce active functional groups into CTFs: Firstly, introducing target functional groups such as C=O, C=N, and N=N during the design of monomers, and then assembling the functional monomers into target CTFs through covalent linkage. This design strategy can precisely control the number of active functional groups and accurately design the structure of CTFs for specific targets. Secondly, synthesizing target CTFs through the groups in existing monomer materials (such as -OH, -CHO, -NH, -CN, *etc.*) and other functional side chains. This post-synthetic modification strategy can also cause structural defects, exposing more active sites and further enhancing performance. Especially for LSBs, specific groups (such as -OH) can improve the conversion rate of Li_xS and limit the shuttle effect.

(3) Exfoliation: Generally, CTFs with high crystallinity have stronger π-π interactions and tighter interlayer arrangement. However, this also leads to a long ion transmission distance and a large transmission resistance. So, it is difficult for ions to penetrate through the channels of CTFs to the active sites inside the

skeleton, which greatly affects the electrochemical performance of CTFs-based electrodes. Interestingly, the interlayer exfoliation can reduce the interlayer stacking density, realize the thin layers of CTFs with small thickness, and shorten the ion diffusion distance, which is an effective strategy for regulating ion diffusion. The current exfoliation strategies are mainly divided into two types of exfoliation methods: physical and chemical.

In short, the above strategies are effective whether it is hybridized with conductive graphene materials, introducing functional groups for customization or regulating the electrochemical properties of CTFs through interface engineering. Within LIBs, the aromatic triazine linkages and robust covalent bonds in CTFs provide stable redox sites for extended cycling, while their porous structure facilitates the diffusion of electrolytes. Beyond the triazine and benzene rings in CTFs, additional nitrogen sites such as secondary and tertiary amines offer further redox sites, enhancing the energy density. In addressing the volumetric expansion issues of SIBs, the rigid and porous architecture of CTFs helps mitigate safety concerns caused by expansion. Furthermore, the insolubility of CTFs enhances the safety of SIBs. Regarding LSBs, the orderly and stable porous structure of CTFs allows for higher sulfur loading, promotes uniform sulfur distribution, and restricts the dissolution of Li_xS, which is crucial in suppressing the "shuttle effect". Additionally, the extra electron pairs in nitrogen and oxygen within CTFs can interact with the strong Lewis acidic sites of terminal lithium atoms in Li_xS, thereby improving electrochemical performance significantly. The introduction of electron-donating or electron-withdrawing groups by screening monomers and the increase of redox active sites can increase the concentration of the active parts of CTF, thereby improving the theoretical specific capacity. In addition to the structural advantages of COFs, the triazine ring in the skeleton also gives CTFs high structural stability and rich nitrogen content. The stability of the structure is conducive to practical applications under extreme conditions, and the rich nitrogen content gives CTFs materials excellent heteroatom effects (HAE) and provides them with rich active centers. In addition, the fully conjugated network of CTFs can promote the transport of electrons and substances. Although considerable progress has been made in the development of positive electrode materials for metal-ion batteries based on CTFs, it still faces some limitations such as low tap density and difficulties in large-scale production.

APPLICATION OF CTFS AS ELECTROLYTES IN SOLID-STATE BATTERIES

According to the classification of solid-state electrolytes (SSEs), solid-state batteries (SSBs) have three mainstream technical routes: polymer[168], oxide[169], and sulfide SSBs[170]. Among them, polymer electrolytes belong to organic electrolytes, while the oxide and sulfide electrolytes belong to inorganic electrolytes. The ideal solid electrolyte materials should have high ionic conductivity, excellent chemical and electrochemical stability to alkali metals, strong inhibition ability of the generation of lithium dendrites and low cost[171]. However, these three major technical routes currently have both the positive and negative effects. None of them can meet the above requirements at the same time, and there are still certain difficulties in technological breakthroughs. Therefore, the electrolyte chemistry has become an important part for SSBs research.

The CTFs are one of promising candidate solutions as organic SSEs due to their tunable structure, functional design, and relatively large Li^+ migration number. Under normal conditions, due to strong Coulomb interactions, the Li^+ components tend to be tightly bound in the CTFs channels in the form of ion pairs or aggregates. Their migration efficiency mainly depends on the concentration of active sites enabling Li^+ to jump and the distance between active sites in pure CTFs electrolyte, namely the Grotthuss mechanism[172]. Hou *et al.* constructed vinyl and triazine-based bifunctional CTFs (V-COF) materials by room temperature synthesis, and obtained poly(ethylene glycol) dimethacrylate/V-CTF (PDM/V-COF) by

covalent polymerization with ether segments [Figure 11][173]. The covalent bond connection method avoids the formation of two-phase interface. The regular one-dimensional pores and triazine-rich structure of V-COF can improve the transmission rate of Li^+. Meanwhile, the urchin-like V-COF can anchor the polymer substrate and improve its mechanical properties. Therefore, the composite solid electrolyte achieves ultra-high ionic conductivity of 5×10^{-5} S cm^{-1} at room temperature and 1×10^{-4} S cm^{-1} at 40 °C. Besides, the assembled symmetric battery exhibits ultra-long lifetime, and can stably cycle for more than 600 h at a current of 0.1 mA cm^{-2} without obvious increase in polarization.

To enhance the ionic conductivity of CTF-based electrolytes, solvents that promote ion migration can be added. In 2020, Shi *et al.* first proposed to improve the safety of lithium metal batteries by preparing quasi-solid-state electrolytes via simple mechanical blending of functionalized CTFs and ionic liquids[174]. The quasi-solid-state electrolyte exhibits high strength and stability due to its strong CTFs skeleton, and effectively inhibits the growth of lithium dendrites. Its ordered pore structure can load a large amount of ionic liquids and construct 3D continuous ion channels to achieve rapid Li^+ conduction and stable deposition of lithium. The cyano functionalization on its surface can effectively promote the dissociation of lithium salts and enhance the stability of ionic liquids. Also, the quasi-solid-state electrolyte is used in lithium metal batteries to exhibit high room temperature ionic conductivity (1.33 mS cm^{-1}), high Li^+ migration number (0.648), excellent electrochemical/cycling stability, good rate specific capacity and effective inhibition of lithium dendrite growth. Although this study has opened up a new and effective method for the research and application of quasi-solid-state batteries, it is not suitable for solving the interface contact and interface stability of CTFs in all-solid-state batteries (ASSBs).

In 2022, Cheng *et al.* successfully synthesized a Novel single-ion conductive nitrogen-hybridized conjugated framework (NCS) electrolyte with a "donor-acceptor" structural unit, whose framework is composed of an electron-withdrawing triazine ring and an electron-donating piperazine ring [Figure 12][175]. The results show that NCS has more outstanding thermal stability and higher ionic conductivity compared with the control sample COFs without triazine structure (TAL). The triazine ring has a strong coordination effect with Li^+, and the strong electrostatic force formed by the piperazine ring. The density functional theory (DFT) simulation results show that COF with an amphoteric structure can effectively dissociate lithium bis(trifluoromethane)sulfonamide (LiTSFI), and the Li^+ generated after the dissociation of the lithium salt is coordinated and complexed with the conjugated electrolyte. Therefore, without the use of solvents, the room-temperature Li^+ conductivity of NCS can reach 1.49 mS·cm^{-1}, and the Li^+ migration number is as high as 0.84. It also shows excellent electrochemical performance when applied to all-solid-state lithium metal batteries, and the capacity retention is 82% after 100 cycles at 0.5 C. This is due to the stronger acidity in the triazine core, which enables stronger coordination with Li^+ and forms more loose ion pairs. In addition, the solid electrolyte prepared in this study has excellent flame retardancy and thermal stability, thus ensuring the safe use of ASSBs.

The insolubility and porous nature of CTFs render them exceptionally suitable as carrier substrates for ionic liquids, thereby facilitating their use as quasi-solid electrolytes. Moreover, the triazine rings within CTFs exhibit a strong coordination interaction with Li^+, which can lower the energy barrier for ion migration, hence achieving noteworthy ionic conductivity. However, despite their commendable performance, most SSEs based on CTFs are currently fabricated through a powder pressing method, resulting in potential brittleness and interfacial issues with electrodes, thus limiting their practical application in flexible and wearable batteries. Therefore, the development of CTF-based SSEs possesses high flexibility.

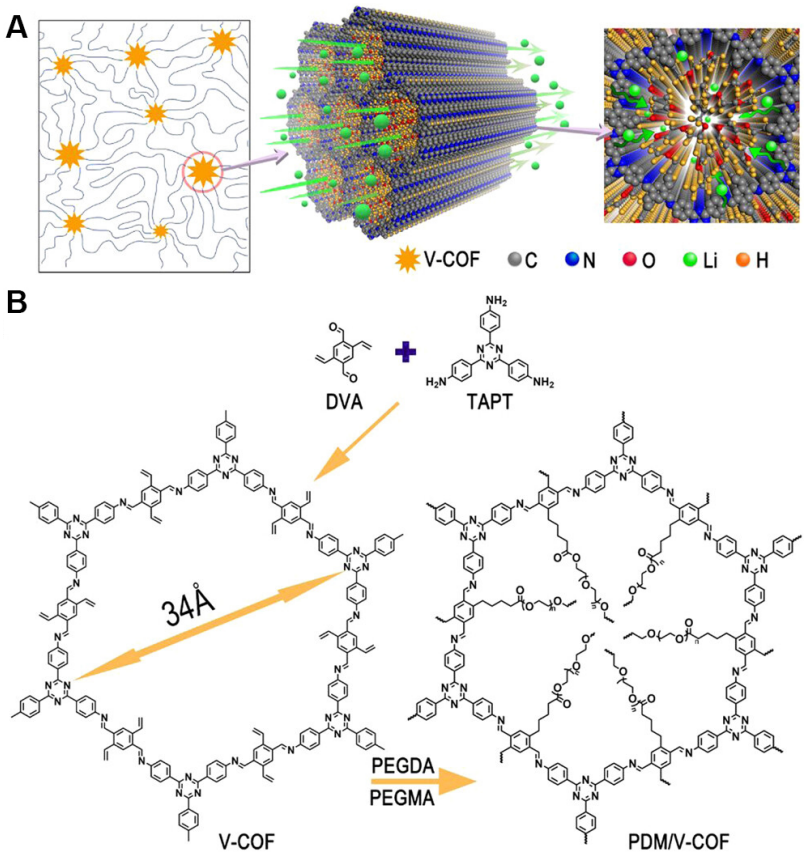

Figure 11. (A) Schematic diagram of Li^+ transport mechanism. (B) Preparation and structure of Vinyl-functionalized CTFs (V-COFs) and PDM/V-COFs[173]. Copyright 2022 John Wiley and Sons.

APPLICATION OF CTFS AS SEPARATOR

Separators are key components in water electrolyzers, fuel cells, metal-ion batteries, electrodialysis and other related processes[176,177]. The efficiency of ion transfer in the separator depends on the energy barrier of ion transfer across the separator. Therefore, constructing efficient ion channels in the separator and reducing the energy barrier of ion transfer across the separator are the key to developing high-performance ion separators. "Microphase Separation" ion separators represented by Nafion membranes have wide ion channels that can efficiently conduct ions, but the ion channels are prone to swelling after absorbing water, resulting in a decrease in the mechanical strength of the separator and a decrease in selectivity and barrier properties[178].

Currently, the widely used separators in metal-ion batteries are polyolefin materials (pore size > 100 nm) and glass fibers (pore size > 450 nm)[179]. These traditional separators are all macroporous materials, which are not conducive to the precise screening of ions. CTFs can easily adjust the geometric size and shape of the pores by selecting different monomers. It can also use molecules with positive or negative charges or no charge to control the number of conductive ions to obtain cationic or anionic conductive membranes. Shi *et al.* first developed a CTF-coated separator for LSBs by simply blade-coating a 2D multilayered CTF onto a Celgard separator[180]. The pore size of CTFs (about 1.2 nm) provides the separator with an ion screening function, selectively allowing Li^+ to pass. The pyridinic/pyrrolic nitrogen in the triazine structure can interact with Li_xS to intercept them, effectively inhibiting their diffusion. Meanwhile, electrochemical impedance spectroscopy (EIS) analysis [Figure 13] shows that the ionic conductivity of the CTF-Celgard

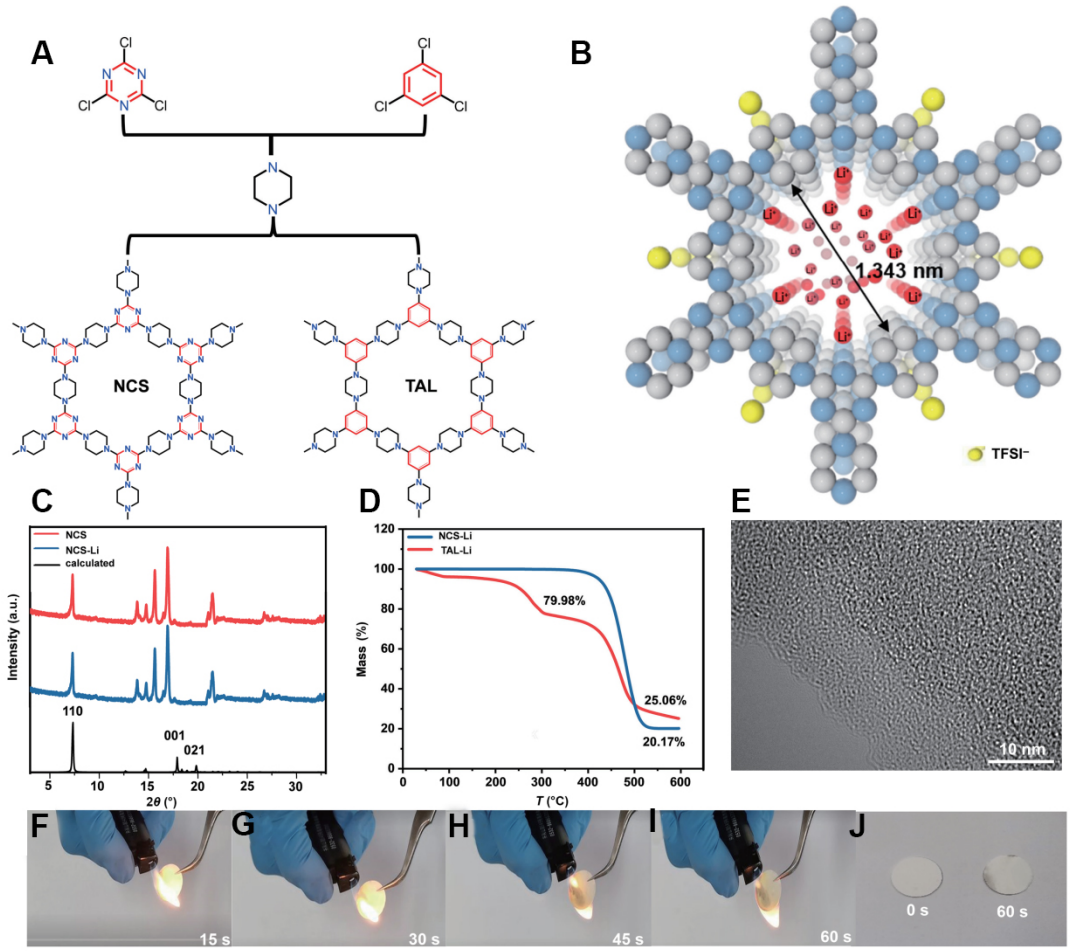

Figure 12. (A) Synthesis of NCS and TAl, (B) Top view of the AA stacking pattern of NCS-Li, (C) PXRD patterns of NCS and NCS-Li, (D) Thermogravimetric images of NCS-Li and TAL-Li, (E) HRTEM image of NCS, and (F-J) Flame retardancy of NCS-Li[175]. Copyright © 2023 Springer Publishing Company.

separator is 0.27 mS cm^{-1} at 30 °C, which is only slightly lower than that of the liquid electrolyte impregnated with the original Celgard separator (0.29 mS cm^{-1}), indicating that the presence of the thin CTFs interlayer has little effect on its conductivity. The commercial separators with CTFs coatings have improved the battery performance, achieving a specific capacity of 1,249 mAh g^{-1} at 0.5 C, an ideal rate performance of 802 mAh g^{-1} at 2 C, and good cycle stability with a capacity decay rate as low as 0.052% per cycle over 800 cycles at 1 C.

In 2021, Shi *et al.* advanced their efforts by employing the electrostatic layer-by-layer self-assembly technique to fabricate an ultralight functional separator with an ordered structure, known as LBL-f separator[181]. This innovative membrane comprises CTFs (CTF@PDDA), enveloped by positively charged poly(diallyldimethylammonium chloride) (PDDA), and negatively charged poly(3,4-ethylenedioxythiophene):poly(styrenesulfonate) (PEDOT:PSS), as presented in Figure 14. The CTF@PDDA layers exhibit robust Li_xS anchoring capability through a combination of physical and chemical interactions, and their substantial specific surface area coupled with a porous configuration enables the enhanced electrolyte absorption. Furthermore, the PEDOT:PSS layer functions as a conductive layer that promotes electron transfer and serves as an exceptional interface stabilizer and adhesive. Consequently, when the

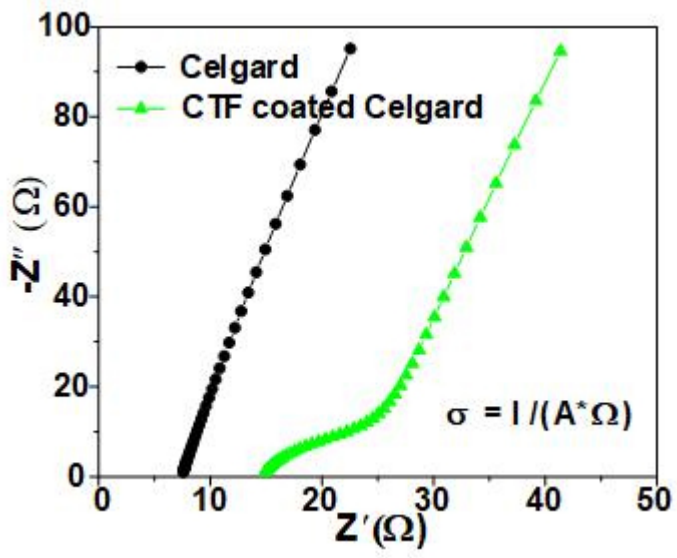

Figure 13. EIS plots of Celgard and CTF-Celgard separators[180]. Copyright © 2019 Elsevier B.V.

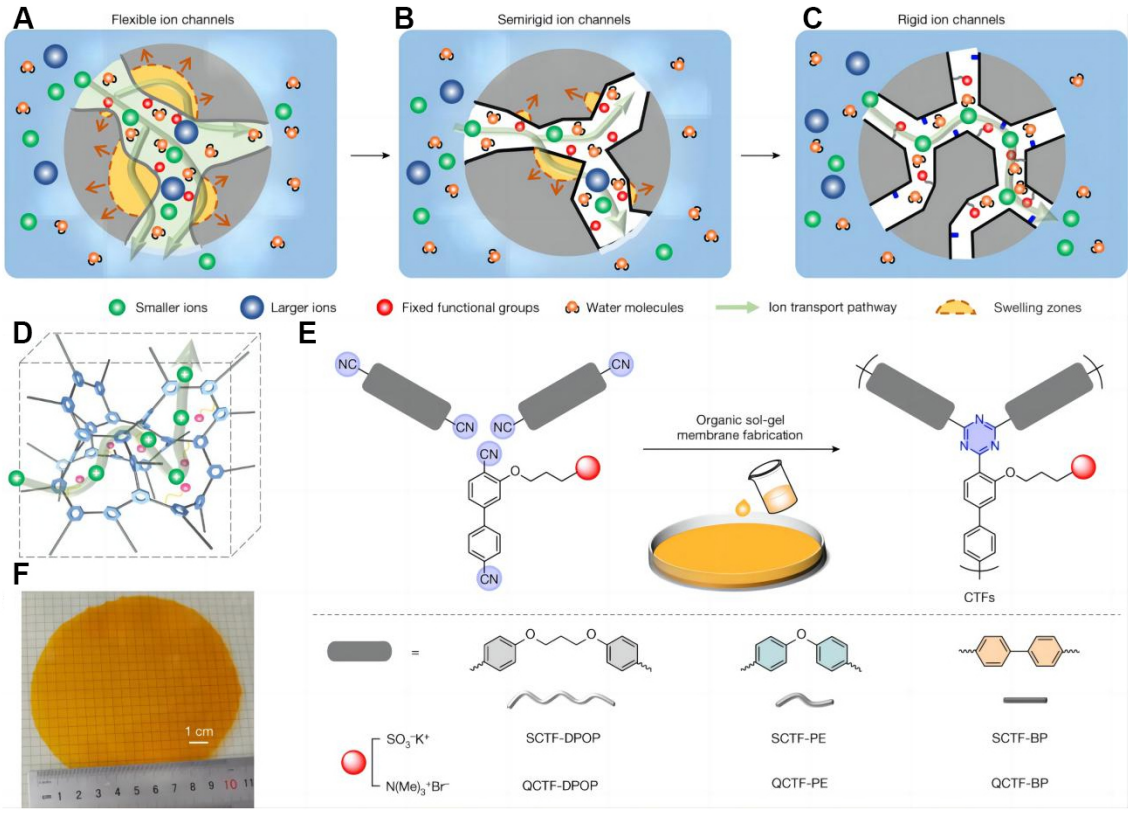

Figure 14. (A-D) Schematic diagram of flexible, semi-rigid, and rigid polymer membrane ion channels, (E) CTF preparation using superacid-catalyzed organic sol-gel reaction, and (F) Free-standing CTF membrane with a diameter of more than 10 cm[182]. Copyright © 2023 Springer Nature.

proposed LBL-f separators are employed in conjunction with standard sulfur cathodes and lithium-metal anodes, they exhibit remarkable cycling stability (capacity decay rate per cycle of 0.052% over 1,000 cycles at

1.0 C), and elevated sulfur utilization rates (90.7% at 0.1 C and 59.2% at 2.0 C). In recent research, Zuo *et al.* have reported a CTF membrane with tunable ionic channel dimensions and chemical properties [Figure 14C and D], which exhibits an exceptionally high ionic diffusion rate and exceedingly low permeability to active materials[182]. The researchers constructed the CTF membrane [Figure 14E and F] by using functional aromatic nitrile monomers through an organic solvent-gelation reaction, where the pore geometry was fine-tuned via different monomers and the chemical characteristics of the pores were regulated by controlling the types and quantities of functional groups, respectively [Figure 14E]. Molecular simulations of the negatively charged CTFs membrane (SCTF) reveal that the SCTF built from rigid monomers (SCTF-BP) displays an accumulated pore volume that is nearly an order of magnitude higher than that of the SCTF constructed from flexible monomers (SCTF-DPOP) [Figure 15A and B]. After force field aging, SCTF-BP retained the most interconnected volume elements, indicative of its enhanced resistance to swelling. The CO_2 adsorption capacity of SCTF-BP is lower than that of classical semi-rigid polymer (PIM) membranes, suggesting a smaller free volume size for SCTF-BP [Figure 15C]. When compared with commercial ion-exchange membranes and reported PIM membranes, the SCTF-BP membrane exhibits an extremely low swelling rate (outlined in Figure 15D). Four-point EIS analysis indicates that the K^+ ion conductivity of the SCTF-BP membrane approaches 30 mS cm^{-1} at 30 °C and 54.9 mS cm^{-1} at 70 °C at a low hydration number, respectively, which is significantly surpassing the other reported PIM membranes [Figure 15E].

The inherent microporous structure of CTFs can enhance the ability of commercial separators to capture Li_xS, thereby augmenting the lifespan and energy density of LSBs. Nevertheless, the mechanical stability of the separators incorporating CTFs may be compromised during operation, potentially leading to cracking. Furthermore, the interfacial resistance between the CTF-modified separators and the electrolyte may increase, resulting in the diminished performance. On another front, the scalability of the production process for CTF-modified separators may present a challenge, necessitating the exploration of alternative methods to disperse CTFs onto the separator to ensure a consistent and uniform coating on the separator surface. Although the preliminary results are promising, the long-term stability and durability of CTF-modified separators require further validation within actual battery systems. Consequently, the sustained research and development are essential to optimize performance and fully elucidate the long-term stability and durability of CTFs.

CONCLUSIONS AND OUTLOOKS

The richness of structural units in CTFs and the diversity of ligands render them a veritable "database" for the development of excellent materials in metal-ion batteries. Their high degree of designability and unique, stable structural characteristics endow them superior ion loading capacity, uniform distribution, rapid transport, and selective affinity. These contributions have been demonstrated in exemplary applications within electrodes, separators, and electrolytes. For instance, CTFs can effectively confine the dissolution of Li_xS, thereby fundamentally enhancing the cycle lifetime of LSBs. However, the sulfur adsorption capacity of conventionally designed CTFs is constrained by their surface area and pore size distribution. Additionally, with the operation of energy storage devices, the CTFs cathodes undergo gradual, irreversible structural disintegration, leading to the detachment of anchored cathode materials from the CTFs matrix, resulting in a decline in the battery performance. Despite the increasing importance of CTFs in the energy storage sector due to the versatility and precision of their synthesis methods, their application in metal-ion batteries remains fraught with challenges [Figure 16].

(1) Small Scale. Although there are synthetic methods for CTFs, such as high-temperature polycondensation and strong acid catalysis, most of them require high temperature, a large amount of catalyst and solvent.

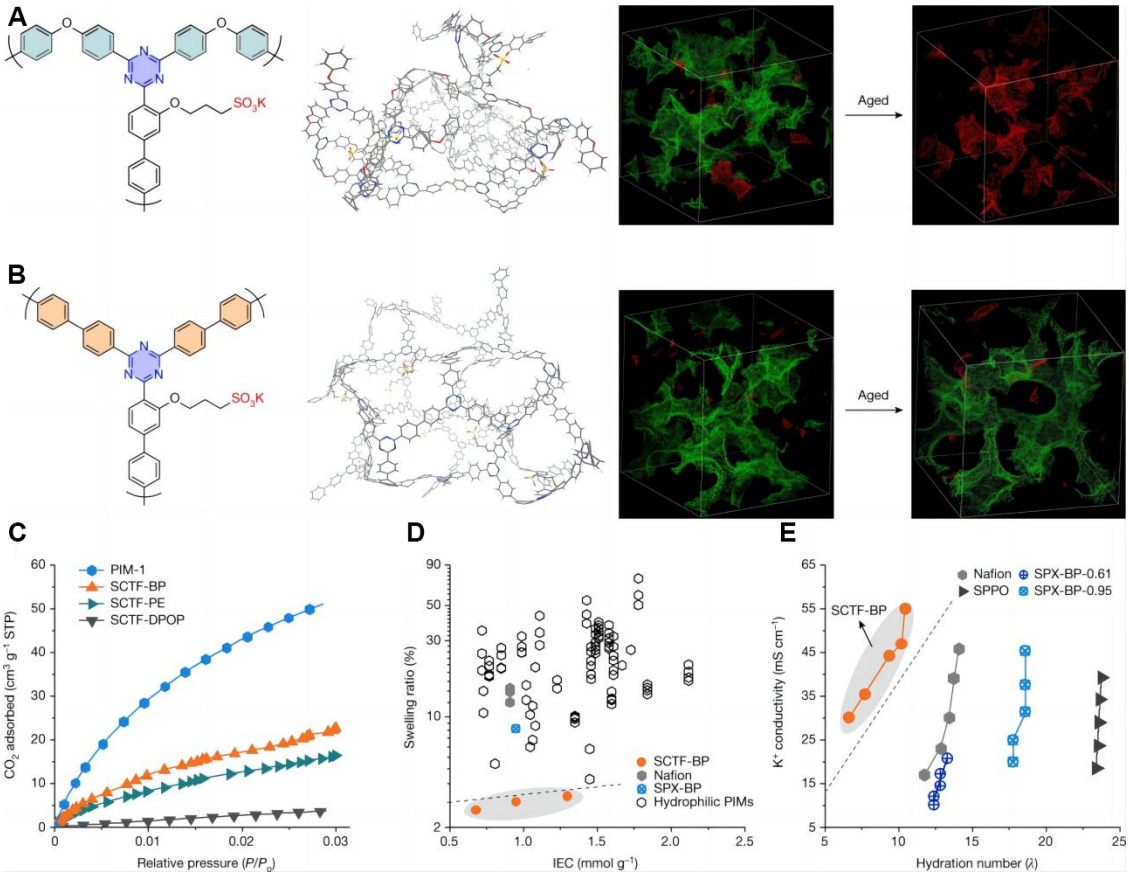

Figure 15. Characterization of negatively charged CTFs membranes (SCTF)[182]. Copyright © 2023 Springer Nature.

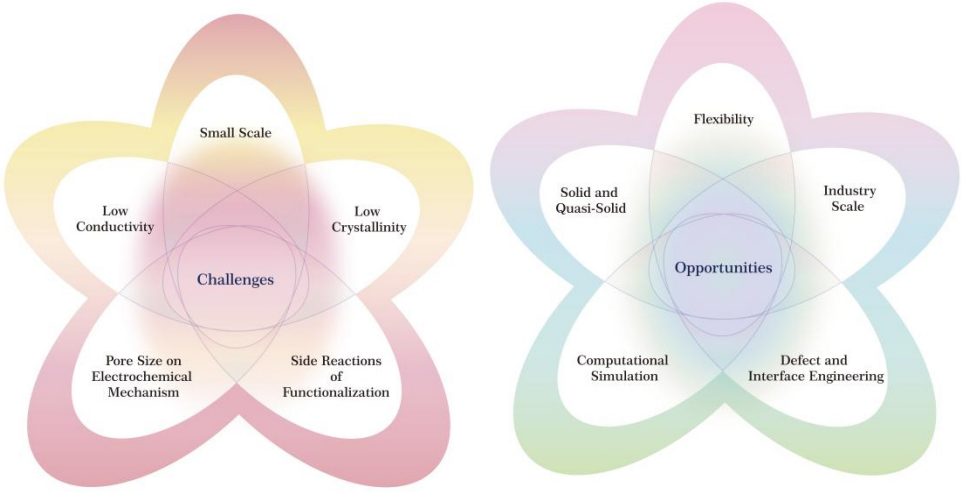

Figure 16. Challenges and opportunities of CTFs.

Such methods require a strict environment, and the synthesis time is relatively long. Therefore, these synthetic methods remain at the laboratory scale which are not universal. Therefore, it is an inevitable trend to explore and optimize low-cost, operable, and high-yield CTFs synthesis strategies for industrial-scale production and commercialization in the CTFs field.

(2) Low Crystallinity. The high stability of the triazine ring will negatively affect the association and separation of bonds during the polymerization reaction, thereby reducing the order of the target materials. Therefore, it is still an urgent issue to find a more gentle method to construct a higher-crystalline CTF.

(3) Side Reactions of Functionalization. Under the chemical functionalization and customization of CTFs, some side reactions are inevitably produced due to the combined effects of different monomers and high temperatures, resulting in a large number of by-products. This side reaction leads to a decrease in the purity of the target CTFs. In addition, the types of active functional groups embedded in the CTFs skeleton are limited.

(4) Low Conductivity. The low conductivity of CTFs is the main factor limiting the development of CTFs as electrodes. Although the ordered pores in CTFs can promote the diffusion of ions, the diffusion rate in COFs is slow due to the long ion transmission path. Secondly, the structures of CTFs monomers are usually composed of aromatic and triazine rings. This structure determines that the chemical bonds of COFs are long, which also limits ion transmission efficiency. Improving the conjugated structure design of the material and introducing conductive media are the main methods at present. However, such approaches are only temporary solutions and cannot improve the energy density of the material itself.

(5) Electrochemical Mechanism. Although the ion transmission and sealing mechanism of CTFs has been widely discussed academically, the difference in electrochemical performance caused by pore size is still unclear. Meanwhile, the complex mechanism between different pore sizes and ion channels still needs to be explored.

Although CTFs face some challenges, their application research is still under the development. The insolubility of CTFs combined with their considerable ion selectivity has the potential for application in quasi-solid-state and solid-state batteries. However, it is still necessary to combine interface engineering and defect engineering to solve the problems of interface contact and exposure of active sites. In addition, there are no application scenarios for flexible CTFs in metal-ion batteries. Therefore, the CTFs with flexibility and high electrochemical performance may be the potential application in extreme scenarios and wearable mobile devices. Moreover, due to the limitations of current synthesis methods and functional group selection, it is urgent to develop large-scale synthesis methods for CTFs materials. At last, the computational simulation plays an important role in promoting the development of reproducible and scalable synthesis methods for industrial-level production and application.

DECLARATIONS

Authors' contributions

Conceived the idea of this manuscript: Zhang B
Wrote the manuscript: Wang Z
Assisted in the collection of literature and scientific research drawings: Zou X
Supervised and guided the academic expression of this work: Lv M
Further revised the logic, grammar, and professionalism of the manuscript: Wang Z, Lv M, Zhang B

Availability of data and materials

Not applicable.

Financial support and sponsorship

This work was supported by the National Natural Science Foundation of China (52373175), High-level Innovative Talents Foundation of Guizhou Province (Grant No. QKHPTRC-GCC[2023]024), Science and Technology Innovation Team of Natural Science Foundation of Guizhou Province (Grant No. CXTD[2023]005), Science and Technology Innovation Team of Higher Education Department of Guizhou Province (Grant No. QJJ[2023]053), and Natural Science Foundation of Guizhou University (GZUTGH[2023]12).

Conflicts of interest

All authors declared that there are no conflicts of interest.

Ethical approval and consent to participate

Not applicable.

Consent for publication

Not applicable.

REFERENCES

1. Wu X, Ma J, Wang J, Zhang X, Zhou G, Liang Z. Progress, key issues, and future prospects for Li-ion battery recycling. *Glob Chall* 2022;6:2200067. DOI PubMed PMC
2. Cui Z, Hu W, Zhang G, Zhang Z, Chen Z. An extended kalman filter based SOC estimation method for Li-ion battery. *Energy Rep* 2022;8:81-7. DOI
3. Bibin C, Vijayaram M, Suriya V, Sai Ganesh R, Soundarraj S. A review on thermal issues in Li-ion battery and recent advancements in battery thermal management system. *Mater Today Proc* 2020;33:116-28. DOI
4. Singh S. Energy crisis and climate change. In: Energy: crises, challenges and solutions, Singh P, Singh S, Kumar G, Baweja P, editors; 2021. pp.1-17. DOI
5. Blakers A, Stocks M, Lu B, Cheng C. A review of pumped hydro energy storage. *Prog Energy* 2021;3:022003. DOI
6. Javed MS, Ma T, Jurasz J, Amin MY. Solar and wind power generation systems with pumped hydro storage: review and future perspectives. *Renew Energy* 2020;148:176-92. DOI
7. Mitali J, Dhinakaran S, Mohamad A. Energy storage systems: a review. *Energy Stor Sav* 2022;1:166-216. DOI
8. Poullikkas A. A comparative overview of large-scale battery systems for electricity storage. *Renew Sustain Energy Rev* 2013;27:778-88. DOI
9. Roscher MA, Vetter J, Sauer DU. Cathode material influence on the power capability and utilizable capacity of next generation lithium-ion batteries. *J Power Sources* 2010;195:3922-7. DOI
10. Gailani A, Mokidm R, El-Dalahmeh M, El-Dalahmeh M, Al-Greer M. Analysis of lithium-ion battery cells degradation based on different manufacturers. In: 55th international universities power engineering conference (UPEC), Turin, Italy, 1-4 Sep 2020. DOI
11. Yan L, Zeng X, Li Z, et al. An innovation: dendrite free quinone paired with $ZnMn_2O_4$ for zinc ion storage. *Mater Today Energy* 2019;13:323-30. DOI
12. Kubota K, Dahbi M, Hosaka T, Kumakura S, Komaba S. Towards K-ion and Na-ion batteries as "beyond li-ion". *Chem Rec* 2018;18:459-79. DOI PubMed
13. Blomgren GE. The development and future of lithium ion batteries. *J Electrochem Soc* 2017;164:A5019-25. DOI
14. Cao L, Li D, Soto FA, et al. Highly reversible aqueous zinc batteries enabled by zincophilic-zincophobic interfacial layers and interrupted hydrogen-bond electrolytes. *Angew Chem Int Ed* 2021;60:18845-51. DOI
15. Goikolea E, Palomares V, Wang S, et al. Na-ion batteries - approaching old and new challenges. *Adv Energy Mater* 2020;10:2002055. DOI
16. Kim J, Elabd A, Chung SY, Coskun A, Choi JW. Covalent triazine frameworks incorporating charged polypyrrole channels for high-performance lithium-sulfur batteries. *Chem Mater* 2020;32:4185-93. DOI
17. Wang C, Wu X, Chen Y, et al. Recognition and application of catalysis in secondary rechargeable batteries. *ACS Catal* 2023;13:10641-50. DOI
18. Fei Z, Xing Y, Dong P, Meng Q, Zhang Y. Efficient direct regeneration of spent $LiCoO_2$ cathode materials by oxidative hydrothermal solution. *JOM* 2023;75:3632-42. DOI

19. Wang Y, Liu K, Wang B. Coating strategies of Ni-rich layered cathode in LIBs. *Chem J Chin Univ* 2021;42:1514-29. DOI
20. Tan A, Wen Y, Huang J, et al. Multiredox tripyridine-triazine molecular cathode for lithium-organic battery. *J Power Sources* 2023;567:232963. DOI
21. Lei Z, Chen X, Sun W, Zhang Y, Wang Y. Exfoliated triazine-based covalent organic nanosheets with multielectron redox for high-performance lithium organic batteries. *Adv Energy Mater* 2019;9:1801010. DOI
22. Lu Y, Chen J. Prospects of organic electrode materials for practical lithium batteries. *Nat Rev Chem* 2020;4:127-42. DOI
23. Jung MH, Ghorpade RV. Polyimide containing tricarbonyl moiety as an active cathode for rechargeable Li-ion batteries. *J Electrochem Soc* 2018;165:A2476. DOI
24. Zhang H, Sun W, Chen X, Wang Y. Few-layered fluorinated triazine-based covalent organic nanosheets for high-performance alkali organic batteries. *ACS Nano* 2019;13:14252-61. DOI
25. Xiong P, Zhang S, Wang R, et al. Covalent triazine frameworks for advanced energy storage: challenges and new opportunities. *Energy Environ Sci* 2023;16:3181-213. DOI
26. Zhao-Karger Z, Gao P, Ebert T, et al. New organic electrode materials for ultrafast electrochemical energy storage. *Adv Mater* 2019;31:e1806599. DOI
27. Zhang S, Han D, Ren S, Xiao M, Wang S, Meng Y. Immobilization strategies of organic electrode materials. *Prog Chem* 2020;32:103-18. DOI
28. Lee S, Hong J, Kang K. Redox-active organic compounds for future sustainable energy storage system. *Adv Energy Mater* 2020;10:2001445. DOI
29. Jia M, Mao C, Niu Y, et al. A selenium-confined porous carbon cathode from silk cocoons for Li-Se battery applications. *RSC Adv* 2015;5:96146-50. DOI
30. Sakaushi K, Nickerl G, Wisser FM, et al. An energy storage principle using bipolar porous polymeric frameworks. *Angew Chem Int Ed* 2012;51:7850-4. DOI
31. Wang B, Yuan F, Wang W, et al. A carbon microtube array with a multihole cross profile: releasing the stress and boosting long-cycling and high-rate potassium ion storage. *J Mater Chem A* 2019;7:25845-52. DOI
32. Chu J, Cheng L, Chen L, Wang HG, Cui F, Zhu G. Integrating multiple redox-active sites and universal electrode-active features into covalent triazine frameworks for organic alkali metal-ion batteries. *Chem Eng J* 2023;451:139016. DOI
33. Wu C, Hu M, Yan X, Shan G, Liu J, Yang J. Azo-linked covalent triazine-based framework as organic cathodes for ultrastable capacitor-type lithium-ion batteries. *Energy Stor Mater* 2021;36:347-54. DOI
34. Yadav D, Subodh, Awasthi SK. Recent advances in the design, synthesis and catalytic applications of triazine-based covalent organic polymers. *Mater Chem Front* 2022;6:1574-605. DOI
35. Srinivasan P, Dhingra K, Kailasam K. A critical insight into porous organic polymers (POPs) and its perspectives for next-generation chemiresistive exhaled breath sensing: a state-of-the-art review. *J Mater Chem A* 2023;11:17418-51. DOI
36. Wang Z, Gu S, Cao L, et al. Redox of dual-radical intermediates in a methylene-linked covalent triazine framework for high-performance lithium-ion batteries. *ACS Appl Mater Interfaces* 2021;13:514-21. DOI
37. Jiang F, Wang Y, Qiu T, et al. Synthesis of biphenyl-linked covalent triazine frameworks with excellent lithium storage performance as anode in lithium ion battery. *J Power Sources* 2022;523:231041. DOI
38. Lv S, He Q, Zhang Y, et al. High performance cathode materials for lithium-ion batteries based on a phenothiazine-based covalent triazine framework. *New J Chem* 2023;47:10911-5. DOI
39. Kuhn P, Antonietti M, Thomas A. Porous, covalent triazine-based frameworks prepared by ionothermal synthesis. *Angew Chem Int Ed* 2008;47:3450-3. DOI PubMed
40. Ren S, Bojdys MJ, Dawson R, et al. Porous, fluorescent, covalent triazine-based frameworks via room-temperature and microwave-assisted synthesis. *Adv Mater* 2012;24:2357-61. DOI
41. Yu SY, Mahmood J, Noh HJ, et al. Direct synthesis of a covalent triazine-based framework from aromatic amides. *Angew Chem Int Ed* 2018;57:8438-42. DOI
42. Zhang W, Li C, Yuan YP, et al. Highly energy- and time-efficient synthesis of porous triazine-based framework: microwave-enhanced ionothermal polymerization and hydrogen uptake. *J Mater Chem* 2010;20:6413-5. DOI
43. Lan ZA, Wu M, Fang Z, et al. Ionothermal synthesis of covalent triazine frameworks in a NaCl-KCl-$ZnCl_2$ eutectic salt for the hydrogen evolution reaction. *Angew Chem Int Ed* 2022;61:e202201482. DOI
44. Sun T, Liang Y, Luo W, Zhang L, Cao X, Xu Y. A general strategy for kilogram-scale preparation of highly crystal-line covalent triazine frameworks. *Angew Chem Int Ed* 2022;61:e202203327. DOI
45. Anderson DR, Holovka JM. Thermally resistant polymers containing the s-triazine ring. *J Polym Sci A-1 Polym Chem* 1966;4:1689-702. DOI
46. Ren S, Zeng D, Zhong H, Wang Y, Qian S, Fang Q. Star-shaped donor-pi-acceptor conjugated oligomers with 1,3,5-triazine cores: convergent synthesis and multifunctional properties. *J Phys Chem B* 2010;114:10374-83. DOI
47. Huang W, Wang ZJ, Ma BC, et al. Hollow nanoporous covalent triazine frameworks via acid vapor-assisted solid phase synthesis for enhanced visible light photoactivity. *J Mater Chem A* 2016;4:7555-9. DOI
48. Ma K, Li J, Liu J, et al. Covalent triazine framework featuring single electron Co^{2+} centered in intact porphyrin units for efficient CO_2 photoreduction. *Appl Surf Sci* 2023;629:157453. DOI
49. Liu J, Zan W, Li K, Yang Y, Bu F, Xu Y. Solution synthesis of semiconducting two-dimensional polymer via trimerization of

carbonitrile. *J Am Chem Soc* 2017;139:11666-9. DOI

50. Zhu X, Tian C, Mahurin SM, et al. A superacid-catalyzed synthesis of porous membranes based on triazine frameworks for CO_2 separation. *J Am Chem Soc* 2012;134:10478-84. DOI
51. Zeng T, Li S, Shen Y, et al. Sodium doping and 3D honeycomb nanoarchitecture: key features of covalent triazine-based frameworks (CTF) organocatalyst for enhanced solar-driven advanced oxidation processes. *Appl Catal B Environ* 2019;257:117915. DOI
52. Zhao W, Hu K, Hu C, Wang X, Yu A, Zhang S. Silica gel microspheres decorated with covalent triazine-based frameworks as an improved stationary phase for high performance liquid chromatography. *J Chromatogr A* 2017;1487:83-8. DOI
53. Bhunia A, Esquivel D, Dey S, et al. A photoluminescent covalent triazine framework: CO_2 adsorption, light-driven hydrogen evolution and sensing of nitroaromatics. *J Mater Chem A* 2016;4:13450-7. DOI
54. Liu J, Lyu P, Zhang Y, Nachtigall P, Xu Y. New layered triazine framework/exfoliated 2D polymer with superior sodium-storage properties. *Adv Mater* 2018;30:1705401. DOI PubMed
55. Wang K, Yang LM, Wang X, et al. Covalent triazine frameworks via a low-temperature polycondensation approach. *Angew Chem Int Ed* 2017;56:14149-53. DOI PubMed PMC
56. Wang H, Qiu N, Kong X, et al. Novel carbazole-based porous organic polymer for efficient iodine capture and rhodamine B adsorption. *ACS Appl Mater Interfaces* 2023;15:14846-53. DOI
57. Han X, Zhao F, Shang Q, Zhao J, Zhong X, Zhang J. Effect of nitrogen atom introduction on the photocatalytic hydrogen evolution activity of covalent triazine frameworks: experimental and theoretical study. *ChemSusChem* 2022;15:e202200828. DOI
58. Asadi P, Taymouri S, Khodarahmi G, et al. Novel nanoscale vanillin based covalent triazine framework as a novel carrier for sustained release of imatinib. *Polym Adv Technol* 2023;34:1358-66. DOI
59. Yildirim O, Derkus B. Triazine-based 2D covalent organic frameworks improve the electrochemical performance of enzymatic biosensors. *J Mater Sci* 2020;55:3034-44. DOI
60. Sharma RK, Yadav P, Yadav M, et al. Recent development of covalent organic frameworks (COFs): synthesis and catalytic (organic-electro-photo) applications. *Mater Horiz* 2020;7:411-54. DOI
61. Wang D, Zheng Z, Hong C, Liu Y, Pan C. Michael addition polymerizations of difunctional amines (AA′) and triacrylamides (B_3). *J Polym Sci A Polym Chem* 2006;44:6226-42. DOI
62. Liu M, Huang Q, Wang S, et al. Crystalline covalent triazine frameworks by in situ oxidation of alcohols to aldehyde monomers. *Angew Chem Int Ed* 2018;57:11968-72. DOI
63. You Q, Wang F, Wu C, et al. Synthesis of 1,3,5-triazines via $Cu(OAc)_2$-catalyzed aerobic oxidative coupling of alcohols and amidine hydrochlorides. *Org Biomol Chem* 2015;13:6723-7. DOI
64. Zha GF, Fang WY, Leng J, Qin HL. A simple, mild and general oxidation of alcohols to aldehydes or ketones by SO_2F_2/K_2CO_3 using DMSO as solvent and oxidant. *Adv Synth Catal* 2019;361:2262-7. DOI
65. Puthiaraj P, Cho SM, Lee YR, Ahn WS. Microporous covalent triazine polymers: efficient friedel-crafts synthesis and adsorption/storage of CO_2 and CH_4. *J Mater Chem A* 2015;3:6792-7. DOI
66. Dey S, Bhunia A, Esquivel D, Janiak C. Covalent triazine-based frameworks (CTFs) from triptycene and fluorene motifs for CO_2 adsorption. *J Mater Chem A* 2016;4:6259-63. DOI
67. Troschke E, Grätz S, Lübken T, Borchardt L. Mechanochemical friedel-crafts alkylation-A sustainable pathway towards porous organic polymers. *Angew Chem Int Ed* 2017;56:6859-63. DOI PubMed
68. Fang XC, Geng TM, Wang FQ, Xu WH. The synthesis of conjugated microporous polymers via Friedel-Crafts reaction of 2,4,6-trichloro-1,3,5-triazine with thienyl derivatives for fluorescence sensing to 2,4-dinitrophenol and capturing iodine. *J Solid State Chem* 2022;307:122818. DOI
69. Lim H, Cha MC, Chang JY. Preparation of microporous polymers based on 1,3,5-triazine units showing high CO_2 adsorption capacity. *Macro Chem Phys* 2012;213:1385-90. DOI
70. Artz J. Covalent triazine-based frameworks - tailor-made catalysts and catalyst supports for molecular and nanoparticulate species. *ChemCatChem* 2018;10:1753-71. DOI
71. Ravi S, Kim J, Choi Y, et al. Metal-free amine-anchored triazine-based covalent organic polymers for selective CO_2 adsorption and conversion to cyclic carbonates under mild conditions. *ACS Sustain Chem Eng* 2023;11:1190-9. DOI
72. Feng G, Yang M, Chen H, Liu B, Liu Y, Li H. Triazine-containing polytriphenylimidazolium network for heterogeneous catalysis of CO_2 conversion to cyclic carbonates. *Sep Purif Technol* 2023;323:124484. DOI
73. Geng TM, Fang XC, Wang FQ, Zhu F. The synthesis of covalent triazine-based frameworks via friedel-crafts reactions of cyanuric chloride with thienyl and carbazolyl derivatives for fluorescence sensing to picric acid, iodine and capturing iodine. *Macro Mater Eng* 2021;306:2100461. DOI
74. Puthiaraj P, Kim SS, Ahn WS. Covalent triazine polymers using a cyanuric chloride precursor via friedel-crafts reaction for CO_2 adsorption/separation. *Chem Eng J* 2016;283:184-92. DOI
75. Rightmire NR, Hanusa TP. Advances in organometallic synthesis with mechanochemical methods. *Dalton Trans* 2016;45:2352-62. DOI PubMed
76. Xu C, De S, Balu AM, Ojeda M, Luque R. Mechanochemical synthesis of advanced nanomaterials for catalytic applications. *Chem Commun* 2015;51:6698-713. DOI PubMed
77. Krusenbaum A, Kraus FJL, Hutsch S, et al. The rapid mechanochemical synthesis of microporous covalent triazine networks: elucidating the role of chlorinated linkers by a solvent-free approach. *Adv Sustain Syst* 2023;7:2200477. DOI

78. Liang Y, Dong H, Aurbach D, Yao Y. Publisher correction: current status and future directions of multivalent metal-ion batteries. *Nat Energy* 2020;5:822. DOI
79. Mishra A, Mehta A, Basu S, et al. Electrode materials for lithium-ion batteries. *Mater Sci Energy Technol* 2018;1:182-7. DOI
80. Ohzuku T, Brodd RJ. An overview of positive-electrode materials for advanced lithium-ion batteries. *J Power Sources* 2007;174:449-56. DOI
81. Wang KX, Li XH, Chen JS. Surface and interface engineering of electrode materials for lithium-ion batteries. *Adv Mater* 2015;27:527-45. DOI PubMed
82. Esser B, Dolhem F, Becuwe M, Poizot P, Vlad A, Brandell D. A perspective on organic electrode materials and technologies for next generation batteries. *J Power Sources* 2021;482:228814. DOI
83. Shen X, Zhang XQ, Ding F, et al. Advanced electrode materials in lithium batteries: retrospect and prospect. *Energy Mater Adv* 2021;2021:1205324. DOI
84. Gong Z, Yang Y. Recent advances in the research of polyanion-type cathode materials for Li-ion batteries. *Energy Environ Sci* 2011;4:3223-42. DOI
85. Xu B, Qian D, Wang Z, Meng YS. Recent progress in cathode materials research for advanced lithium ion batteries. *Mater Sci Eng R Rep* 2012;73:51-65. DOI
86. He W, Guo W, Wu H, et al. Challenges and recent advances in high capacity Li-rich cathode materials for high energy density lithium-ion batteries. *Adv Mater* 2021;33:e2005937. DOI
87. Lee W, Muhammad S, Sergey C, et al. Advances in the cathode materials for lithium rechargeable batteries. *Angew Chem Int Ed* 2020;59:2578-605. DOI
88. Kraytsberg A, Ein-Eli Y. Higher, stronger, better... a review of 5 volt cathode materials for advanced lithium-ion batteries. *Adv Energy Mater* 2012;2:922-39. DOI
89. Li M, Lu J, Chen Z, Amine K. 30 years of lithium-ion batteries. *Adv Mater* 2018;30:e1800561. DOI
90. Wang R, Wang L, Fan Y, Yang W, Zhan C, Liu G. Controversy on necessity of cobalt in nickel-rich cathode materials for lithium-ion batteries. *J Ind Eng Chem* 2022;110:120-30. DOI
91. Su Y, Liu Y, Liu P, et al. Compact coupled graphene and porous polyaryltriazine-derived frameworks as high performance cathodes for lithium-ion batteries. *Angew Chem Int Ed* 2015;54:1812-6. DOI
92. See KA, Hug S, Schwinghammer K, et al. Lithium charge storage mechanisms of cross-linked triazine networks and their porous carbon derivatives. *Chem Mater* 2015;27:3821-9. DOI
93. Woo SW, Dokko K, Nakano H, Kanamura K. Preparation of three dimensionally ordered macroporous carbon with mesoporous walls for electric double-layer capacitors. *J Mater Chem* 2008;18:1674-80. DOI
94. Wang DW, Li F, Liu M, Lu GQ, Cheng HM. 3D aperiodic hierarchical porous graphitic carbon material for high-rate electrochemical capacitive energy storage. *Angew Chem Int Ed* 2008;47:373-6. DOI
95. Liu HJ, Wang J, Wang CX, Xia YY. Ordered hierarchical mesoporous/microporous carbon derived from mesoporous titanium-carbide/carbon composites and its electrochemical performance in supercapacitor. *Adv Energy Mater* 2011;1:1101-8. DOI
96. Liu HJ, Wang XM, Cui WJ, Dou YQ, Zhao DY, Xia YY. Highly ordered mesoporous carbon nanofiber arrays from a crab shell biological template and its application in supercapacitors and fuel cells. *J Mater Chem* 2010;20:4223-30. DOI
97. Yuan R, Kang W, Zhang C. Rational design of porous covalent triazine-based framework composites as advanced organic lithium-ion battery cathodes. *Materials* 2018;11:937. DOI PubMed PMC
98. Yang DH, Yao ZQ, Wu D, Zhang YH, Zhou Z, Bu XH. Structure-modulated crystalline covalent organic frameworks as high-rate cathodes for Li-ion batteries. *J Mater Chem A* 2016;4:18621-7. DOI
99. Wang S, Wang Q, Shao P, et al. Exfoliation of covalent organic frameworks into few-layer redox-active nanosheets as cathode materials for lithium-ion batteries. *J Am Chem Soc* 2017;139:4258-61. DOI
100. Xu F, Jin S, Zhong H, et al. Electrochemically active, crystalline, mesoporous covalent organic frameworks on carbon nanotubes for synergistic lithium-ion battery energy storage. *Sci Rep* 2015;5:8225. DOI PubMed PMC
101. Jiao L, Hu Y, Ju H, et al. From covalent triazine-based frameworks to N-doped porous carbon/reduced graphene oxide nanosheets: efficient electrocatalysts for oxygen reduction. *J Mater Chem A* 2017;5:23170-8. DOI
102. Zhu J, Zhuang X, Yang J, Feng X, Hirano S. Graphene-coupled nitrogen-enriched porous carbon nanosheets for energy storage. *J Mater Chem A* 2017;5:16732-9. DOI
103. Guan R, Zhong L, Wang S, et al. Synergetic covalent and spatial confinement of sulfur species by phthalazinone-containing covalent triazine frameworks for ultrahigh performance of Li-S batteries. *ACS Appl Mater Interfaces* 2020;12:8296-305. DOI
104. Haldar S, Roy K, Kushwaha R, Ogale S, Vaidhyanathan R. Chemical exfoliation as a controlled route to enhance the anodic performance of COF in LIB. *Adv Energy Mater* 2019;9:1902428. DOI
105. Wang Z, Li Y, Liu P, et al. Few layer covalent organic frameworks with graphene sheets as cathode materials for lithium-ion batteries. *Nanoscale* 2019;11:5330-5. DOI
106. Zhao G, Li H, Gao Z, et al. Dual-active-center of polyimide and triazine modified atomic-layer covalent organic frameworks for high-performance Li storage. *Adv Funct Mater* 2021;31:2101019. DOI
107. Ma T, Zhao Q, Wang J, Pan Z, Chen J. A sulfur heterocyclic quinone cathode and a multifunctional binder for a high-performance rechargeable lithium-ion battery. *Angew Chem Int Ed* 2016;55:6428-32. DOI
108. Peng C, Ning GH, Su J, et al. Reversible multi-electron redox chemistry of π-conjugated N-containing heteroaromatic molecule-

based organic cathodes. *Nat Energy* 2017;2:1-9. DOI

109. Luo C, Ji X, Hou S, et al. Azo compounds derived from electrochemical reduction of nitro compounds for high performance Li-ion batteries. *Adv Mater* 2018;30:e1706498. DOI
110. Chen X, Zhang H, Yan P, et al. Bipolar fluorinated covalent triazine framework cathode with high lithium storage and long cycling capability. *RSC Adv* 2022;12:11484-91. DOI PubMed PMC
111. Li Y, Zheng S, Liu X, et al. Conductive microporous covalent triazine-based framework for high-performance electrochemical capacitive energy storage. *Angew Chem Int Ed* 2018;57:7992-6. DOI
112. Liu W, Wang K, Zhan X, et al. Highly connected three-dimensional covalent organic framework with flu topology for high-performance Li-S batteries. *J Am Chem Soc* 2023;145:8141-9. DOI
113. Xu J, Zhu C, Song S, Fang Q, Zhao J, Shen Y. A nanocubicle-like 3D adsorbent fabricated by in situ growth of 2D heterostructures for removal of aromatic contaminants in water. *J Hazard Mater* 2022;423:127004. DOI
114. Ren L, Lian L, Zhang X, et al. Boosting lithium storage in covalent triazine framework for symmetric all-organic lithium-ion batteries by regulating the degree of spatial distortion. *J Colloid Interface Sci* 2024;660:1039-47. DOI
115. Sakaushi K, Hosono E, Nickerl G, et al. Aromatic porous-honeycomb electrodes for a sodium-organic energy storage device. *Nat Commun* 2013;4:1485. DOI
116. Xu H, Yan Q, Yao W, Lee CS, Tang Y. Mainstream optimization strategies for cathode materials of sodium-ion batteries. *Small Struct* 2022;3:2100217. DOI
117. Liu Q, Hu Z, Li W, et al. Sodium transition metal oxides: the preferred cathode choice for future sodium-ion batteries? *Energy Environ Sci* 2021;14:158-79. DOI
118. Perveen T, Siddiq M, Shahzad N, Ihsan R, Ahmad A, Shahzad MI. Prospects in anode materials for sodium ion batteries - a review. *Renew Sustain Energy Rev* 2020;119:109549. DOI
119. Yang C, Xin S, Mai L, You Y. Materials Design for high-safety sodium-ion battery. *Adv Energy Mater* 2021;11:2000974. DOI
120. Li K, Wang Y, Gao B, Lv X, Si Z, Wang HG. Conjugated microporous polyarylimides immobilization on carbon nanotubes with improved utilization of carbonyls as cathode materials for lithium/sodium-ion batteries. *J Colloid Interface Sci* 2021;601:446-53. DOI
121. Shi J, Tang W, Xiong B, Gao F, Lu Q. Molecular design and post-synthetic vulcanization on two-dimensional covalent organic framework@rGO hybrids towards high-performance sodium-ion battery cathode. *Chem Eng J* 2023;453:139607. DOI
122. Sun R, Hou S, Luo C, et al. A covalent organic framework for fast-charge and durable rechargeable Mg storage. *Nano Lett* 2020;20:3880-8. DOI
123. Pan B, Huang J, Feng Z, et al. Polyanthraquinone-based organic cathode for high-performance rechargeable magnesium-ion batteries. *Adv Energy Mater* 2016;6:1600140. DOI
124. Dong H, Liang Y, Tutusaus O, et al. Directing Mg-storage chemistry in organic polymers toward high-energy Mg batteries. *Joule* 2019;3:782-93. DOI
125. Leisegang T, Meutzner F, Zschornak M, et al. The aluminum-ion battery: a sustainable and seminal concept? *Front Chem* 2019;7:268. DOI PubMed PMC
126. Yuan D, Zhao J, Manalastas Jr. W, Kumar S, Srinivasan M. Emerging rechargeable aqueous aluminum ion battery: status, challenges, and outlooks. *Nano Mater Sci* 2020;2:248-63. DOI
127. Jayaprakash N, Das SK, Archer LA. The rechargeable aluminum-ion battery. *Chem Commun* 2011;47:12610-2. DOI PubMed
128. Meng J, Zhu L, Haruna AB, Ozoemena KI, Pang Q. Charge storage mechanisms of cathode materials in rechargeable aluminum batteries. *Sci China Chem* 2021;64:1888-907. DOI
129. Liu Y, Lu Y, Hossain Khan A, et al. Redox-bipolar polyimide two-dimensional covalent organic framework cathodes for durable aluminium batteries. *Angew Chem Int Ed* 2023;62:e202306091. DOI
130. Tang B, Shan L, Liang S, Zhou J. Issues and opportunities facing aqueous zinc-ion batteries. *Energy Environ Sci* 2019;12:3288-304. DOI
131. Fang G, Zhou J, Pan A, Liang S. Recent advances in aqueous zinc-ion batteries. *ACS Energy Lett* 2018;3:2480-501. DOI
132. Jia X, Liu C, Neale ZG, Yang J, Cao G. Active materials for aqueous zinc ion batteries: synthesis, crystal structure, morphology, and electrochemistry. *Chem Rev* 2020;120:7795-866. DOI
133. Wang Y, Wang X, Tang J, Tang W. A quinoxalinophenazinedione covalent triazine framework for boosted high-performance aqueous zinc-ion batteries. *J Mater Chem A* 2022;10:13868-75. DOI
134. Gao X, Sha Y, Lin Q, Cai R, Tade MO, Shao Z. Combustion-derived nanocrystalline $LiMn_2O_4$ as a promising cathode material for lithium-ion batteries. *J Power Sources* 2015;275:38-44. DOI
135. Mikhaylik YV, Akridge JR. Polysulfide shuttle study in the Li/S battery system. *J Electrochem Soc* 2004;151:A1969. DOI
136. Zhao M, Li BQ, Zhang XQ, Huang JQ, Zhang Q. A perspective toward practical lithium-sulfur batteries. *ACS Cent Sci* 2020;6:1095-104. DOI PubMed PMC
137. Manthiram A, Fu Y, Su YS. Challenges and prospects of lithium-sulfur batteries. *ACC Chem Res* 2013;46:1125-34. DOI PubMed
138. Manthiram A, Chung SH, Zu C. Lithium-sulfur batteries: progress and prospects. *Adv Mater* 2015;27:1980-2006. DOI PubMed
139. Seh ZW, Sun Y, Zhang Q, Cui Y. Designing high-energy lithium-sulfur batteries. *Chem Soc Rev* 2016;45:5605-34. DOI
140. Ma L, Zhuang HL, Wei S, et al. Enhanced Li-S batteries using amine-functionalized carbon nanotubes in the cathode. *ACS Nano* 2016;10:1050-9. DOI

141. Zhang T, Zhang L, Zhao L, Huang X, Hou Y. Catalytic effects in the cathode of Li-S batteries: accelerating polysulfides redox conversion. *EnergyChem* 2020;2:100036. DOI
142. Khazraji MR, Wang J, Wei S. Recent progress of anode protection in Li-S batteries. *Energy Technol* 2023;11:2200944. DOI
143. Jeong YC, Kim JH, Nam S, Park CR, Yang SJ. Rational design of nanostructured functional interlayer/separator for advanced Li-S batteries. *Adv Funct Mater* 2018;28:1707411. DOI
144. Pathak D, Mandal BP, Tyagi AK. A new strategic approach to modify electrode and electrolyte for high performance Li-S battery. *J Power Sources* 2021;488:229456. DOI
145. Li J, Chen C, Chen Y, et al. Polysulfide confinement and highly efficient conversion on hierarchical mesoporous carbon nanosheets for Li-S batteries. *Adv Energy Mater* 2019;9:1901935. DOI
146. Pei F, An T, Zang J, et al. From hollow carbon spheres to N-doped hollow porous carbon bowls: rational design of hollow carbon host for Li-S batteries. *Adv Energy Mater* 2016;6:1502539. DOI
147. Chen M, Su Z, Jiang K, Pan Y, Zhang Y, Long D. Promoting sulfur immobilization by a hierarchical morphology of hollow carbon nanosphere clusters for high-stability Li-S battery. *J Mater Chem A* 2019;7:6250-8. DOI
148. Luo D, Li M, Ma Q, et al. Porous organic polymers for Li-chemistry-based batteries: functionalities and characterization studies. *Chem Soc Rev* 2022;51:2917-38. DOI
149. Liao H, Ding H, Li B, Ai X, Wang C. Covalent-organic frameworks: potential host materials for sulfur impregnation in lithium-sulfur batteries. *J Mater Chem A* 2014;2:8854-8. DOI
150. Talapaneni SN, Hwang TH, Je SH, Buyukcakir O, Choi JW, Coskun A. Elemental-sulfur-mediated facile synthesis of a covalent triazine framework for high-performance lithium-sulfur batteries. *Angew Chem Int Ed* 2016;55:3106-11. DOI PubMed
151. Choi JW, Aurbach D. Promise and reality of post-lithium-ion batteries with high energy densities. *Nat Rev Mater* 2016;1:1-16. DOI
152. Je SH, Kim HJ, Kim J, Choi JW, Coskun A. Perfluoroaryl-elemental sulfur S_NAr chemistry in covalent triazine frameworks with high sulfur contents for lithium-sulfur batteries. *Adv Funct Mater* 2017;27:1703947. DOI
153. Wang DG, Tan L, Wang H, Song M, Wang J, Kuang GC. Multiple covalent triazine frameworks with strong polysulfide chemisorption for enhanced lithium-sulfur batteries. *ChemElectroChem* 2019;6:2777-81. DOI
154. Hou TZ, Xu WT, Chen X, Peng HJ, Huang JQ, Zhang Q. Lithium bond chemistry in lithium-sulfur batteries. *Angew Chem Int Ed* 2017;56:8178-82. DOI
155. Ren X, Liu Z, Zhang M, Li D, Yuan S, Lu C. Review of cathode in advanced Li-S batteries: the effect of doping atoms at micro levels. *ChemElectroChem* 2021;8:3457-71. DOI
156. Li M, Wang Y, Sun S, Yang Y, Gu G, Zhang Z. Rational design of an Allyl-rich Triazine-based covalent organic framework host used as efficient cathode materials for Li-S batteries. *Chem Eng J* 2022;429:132254. DOI
157. Jiang Q, Li Y, Zhao X, et al. Inverse-vulcanization of vinyl functionalized covalent organic frameworks as efficient cathode materials for Li-S batteries. *J Mater Chem A* 2018;6:17977-81. DOI
158. Xu J, An S, Song X, et al. Towards high performance Li-S batteries via sulfonate-rich COF-modified separator. *Adv Mater* 2021;33:e2105178. DOI
159. Zhang Y, Guo C, Zhou J, et al. Anisotropically hybridized porous crystalline Li-S battery separators. *Small* 2023;19:e2206616. DOI
160. Hu X, Jian J, Fang Z, et al. Hierarchical assemblies of conjugated ultrathin COF nanosheets for high-sulfur-loading and long-lifespan lithium-sulfur batteries: fully-exposed porphyrin matters. *Energy Stor Mater* 2019;22:40-7. DOI
161. Xiao Z, Li L, Tang Y, et al. Covalent organic frameworks with lithiophilic and sulfiphilic dual linkages for cooperative affinity to polysulfides in lithium-sulfur batteries. *Energy Stor Mater* 2018;12:252-9. DOI
162. Liang Y, Xia T, Chang Z, et al. Boric acid functionalized triazine-based covalent organic frameworks with dual-function for selective adsorption and lithium-sulfur battery cathode. *Chem Eng J* 2022;437:135314. DOI
163. Mullangi D, Chakraborty D, Pradeep A, et al. Highly stable COF-supported $Co/Co(OH)_2$ nanoparticles heterogeneous catalyst for reduction of nitrile/nitro compounds under mild conditions. *Small* 2018;14:e1801233. DOI
164. Zhang T, Hu F, Song C, et al. Constructing covalent triazine-based frameworks to explore the effect of heteroatoms and pore structure on electrochemical performance in Li-S batteries. *Chem Eng J* 2021;407:127141. DOI
165. Gomes R, Bhattacharyya AJ. Carbon nanotube-templated covalent organic framework nanosheets as an efficient sulfur host for room-temperature metal-sulfur batteries. *ACS Sustain Chem Eng* 2020;8:5946-53. DOI
166. Li W, Zhang Q, Zheng G, Seh ZW, Yao H, Cui Y. Understanding the role of different conductive polymers in improving the nanostructured sulfur cathode performance. *Nano Lett* 2013;13:5534-40. DOI
167. Cao Y, Qi X, Hu K, et al. Conductive polymers encapsulation to enhance electrochemical performance of Ni-rich cathode materials for Li-ion batteries. *ACS Appl Mater Interfaces* 2018;10:18270-80. DOI
168. Wu F, Zhang K, Liu Y, et al. Polymer electrolytes and interfaces toward solid-state batteries: recent advances and prospects. *Energy Stor Mater* 2020;33:26-54. DOI
169. Shoji M, Cheng EJ, Kimura T, Kanamura K. Recent progress for all solid state battery using sulfide and oxide solid electrolytes. *J Phys D Appl Phys* 2019;52:103001. DOI
170. Wu J, Liu S, Han F, Yao X, Wang C. Lithium/sulfide all-solid-state batteries using sulfide electrolytes. *Adv Mater* 2021;33:e2000751. DOI
171. Liu H, Liang Y, Wang C, et al. Priority and prospect of sulfide-based solid-electrolyte membrane. *Adv Mater* 2023;35:e2206013. DOI

172. Guan L, Guo Z, Zhou Q, et al. A highly proton conductive perfluorinated covalent triazine framework via low-temperature synthesis. *Nat Commun* 2023;14:8114. DOI PubMed PMC
173. Hou Z, Xia S, Niu C, et al. Tailoring the interaction of covalent organic framework with the polyether matrix toward high-performance solid-state lithium metal batteries. *Carbon Energy* 2022;4:506-16. DOI
174. Shi QX, Guan X, Pei HJ, et al. Functional covalent triazine frameworks-based quasi-solid-state electrolyte used to enhance lithium metal battery safety. *Batteries Supercaps* 2020;3:936-45. DOI
175. Cheng Z, Lu L, Zhang S, et al. Amphoteric covalent organic framework as single Li^+ superionic conductor in all-solid-state. *Nano Res* 2023;16:528-35. DOI
176. Aili D, Kraglund MR, Rajappan SC, et al. Electrode separators for the next-generation alkaline water electrolyzers. *ACS Energy Lett* 2023;8:1900-10. DOI PubMed PMC
177. Henkensmeier D, Cho WC, Jannasch P, et al. Separators and membranes for advanced alkaline water electrolysis. *Chem Rev* 2024;124:6393-443. DOI PubMed PMC
178. Palanisamy G, Thangarasu S, Dharman RK, et al. The growth of biopolymers and natural earthen sources as membrane/separator materials for microbial fuel cells: a comprehensive review. *J Energy Chem* 2023;80:402-31. DOI
179. Zhu J, Yanilmaz M, Fu K, et al. Understanding glass fiber membrane used as a novel separator for lithium-sulfur batteries. *J Membr Sci* 2016;504:89-96. DOI
180. Shi QX, Pei HJ, You N, et al. Large-scaled covalent triazine framework modified separator as efficient inhibit polysulfide shuttling in Li-S batteries. *Chem Eng J* 2019;375:121977. DOI
181. Shi QX, Yang CY, Pei HJ, et al. Layer-by-layer self-assembled covalent triazine framework/electrical conductive polymer functional separator for Li-S battery. *Chem Eng J* 2021;404:127044. DOI
182. Zuo P, Ye C, Jiao Z, et al. Near-frictionless ion transport within triazine framework membranes. *Nature* 2023;617:299-305. DOI PubMed PMC
183. Yang Z, Wang T, Chen H, et al. Surpassing the organic cathode performance for lithium-ion batteries with robust fluorinated covalent quinazoline networks. *ACS Energy Lett* 2021;6:41-51. DOI
184. Jiang K, Peng P, Tranca D, et al. Covalent triazine frameworks and porous carbons: perspective from an azulene-based case. *Macromol Rapid Commun* 2022;43:e2200392. DOI
185. Geng Q, Xu Z, Wang J, Song C, Wu Y, Wang Y. Tailoring covalent triazine frameworks anode for superior Lithium-ion storage via thioether engineering. *Chem Eng J* 2023;469:143941. DOI
186. Shan J, Liu Y, Su Y, et al. Graphene-directed two-dimensional porous carbon frameworks for high-performance lithium-sulfur battery cathodes. *J Mater Chem A* 2016;4:314-20. DOI
187. Xu F, Yang S, Jiang G, Ye Q, Wei B, Wang H. Fluorinated, sulfur-rich, covalent triazine frameworks for enhanced confinement of polysulfides in lithium-sulfur batteries. *ACS Appl Mater Interfaces* 2017;9:37731-8. DOI
188. Yang S, Liu Q, Lu Q, et al. A facile strategy to improve the electrochemical performance of porous organic polymer-based lithium-sulfur batteries. *Energy Technol* 2019;7:1900583. DOI
189. Feng X, Huang X, Ma Y, Song G, Li H. New structural carbons via industrial gas explosion for hybrid cathodes in Li-S batteries. *ACS Sustain Chem Eng* 2019;7:12948-54. DOI
190. Troschke E, Kensy C, Haase F, et al. Mechanistic insights into the role of covalent triazine frameworks as cathodes in lithium-sulfur batteries. *Batteries Supercaps* 2020;3:1069-79. DOI
191. Yan Y, Chen Z, Yang J, et al. Controllable substitution of S radicals on triazine covalent framework to expedite degradation of polysulfides. *Small* 2020;16:e2004631. DOI
192. Liu XF, Chen H, Wang R, Zang SQ, Mak TCW. Cationic covalent-organic framework as efficient redox motor for high-performance lithium-sulfur batteries. *Small* 2020;16:e2002932. DOI
193. Meng R, Deng Q, Peng C, et al. Two-dimensional organic-inorganic heterostructures of in situ-grown layered COF on Ti_3C_2 MXene nanosheets for lithium-sulfur batteries. *Nano Today* 2020;35:100991. DOI
194. Liang Y, Xia M, Zhao Y, et al. Functionalized triazine-based covalent organic frameworks containing quinoline via aza-Diels-Alder reaction for enhanced lithium-sulfur batteries performance. *J Colloid Interface Sci* 2022;608:652-61. DOI
195. Gao G, Jia Y, Gao H, et al. New covalent triazine framework rich in nitrogen and oxygen as a host material for lithium-sulfur batteries. *ACS Appl Mater Interfaces* 2021;13:50258-69. DOI
196. Fan X, Chen S, Gong W, et al. A conjugated porous polymer complexed with a single-atom cobalt catalyst as an electrocatalytic sulfur host for enhancing cathode reaction kinetics. *Energy Stor Mater* 2021;41:14-23. DOI
197. Wu C, Yan X, Yu H, et al. Engineering strong electronegative nitrogen-rich porous organic polymer for practical durable lithium-sulfur battery. *J Power Sources* 2022;551:232212. DOI
198. Senthil C, Jung HY. Molecular polysulfide-scavenging sulfurized-triazine polymer enable high energy density Li-S battery under lean electrolyte. *Energy Stor Mater* 2023;55:225-35. DOI
199. Yang Z, Hu Z, Yan G, et al. Multi-function hollow nanorod as an efficient sulfur host accelerates sulfur redox reactions for high-performance Li-S batteries. *J Colloid Interface Sci* 2023;629:65-75. DOI
200. Cao Y, Jia Y, Meng X, et al. Covalently grafting conjugated porous polymers to MXene offers a two-dimensional sandwich-structured electrocatalytic sulfur host for lithium-sulfur batteries. *Chem Eng J* 2022;446:137365. DOI
201. Yan R, Mishra B, Traxler M, et al. A thiazole-linked covalent organic framework for lithium-sulphur batteries. *Angew Chem Int Ed*

2023;62:e202302276. DOI

202. Mahato M, Nam S, Lee MJ, Koratkar N, Oh IK. Physicochemically interlocked sulfur covalent triazine framework for lithium-sulfur batteries with exceptional longevity. *Small* 2023;19:e2301847. DOI